MCB
Journals.ASM.org

Impact of CUX2 on the Female Mouse Liver Transcriptome: Activation of Female-Biased Genes and Repression of Male-Biased Genes

Tara L. Conforto, Yijing Zhang, Jennifer Sherman, and David J. Waxman

Division of Cell and Molecular Biology, Department of Biology, Boston University, Boston, Massachusetts, USA

The growth hormone-regulated transcription factors STAT5 and BCL6 coordinately regulate sex differences in mouse liver, primarily through effects in male liver, where male-biased genes are upregulated and many female-biased genes are actively repressed. Here we investigated whether CUX2, a highly female-specific liver transcription factor, contributes to an analogous regulatory network in female liver. Adenoviral overexpression of CUX2 in male liver induced 36% of female-biased genes and repressed 35% of male-biased genes. In female liver, CUX2 small interfering RNA (siRNA) preferentially induced genes repressed by adenovirus expressing CUX2 (adeno-CUX2) in male liver, and it preferentially repressed genes induced by adeno-CUX2 in male liver. CUX2 binding in female liver chromatin was enriched at sites of male-biased DNase hypersensitivity and at genomic regions showing male-enriched STAT5 binding. CUX2 binding was also enriched near genes repressed by adeno-CUX2 in male liver or induced by CUX2 siRNA in female liver but not at genes induced by adeno-CUX2, indicating that CUX2 binding is preferentially associated with gene repression. Nevertheless, direct CUX2 binding was seen at several highly female-specific genes that were positively regulated by CUX2, including *A1bg*, *Cyp2b9*, *Cyp3a44*, *Tox*, and *Trim24*. CUX2 expression and chromatin binding were high in immature male liver, where repression of adult male-biased genes and expression of adult female-biased genes are common, suggesting that the downregulation of CUX2 in male liver at puberty contributes to the developmental changes establishing adult patterns of sex-specific gene expression.

Sex differences in liver gene expression are widespread and affect a broad range of physiological processes, including steroid and drug metabolism, pheromone binding, and lipid metabolism. Hepatic sex-biased genes are regulated by growth hormone (GH) (35, 49), which is secreted by the pituitary gland in a sex-specific manner in rats, mice, and humans (16, 28, 44, 53). Pituitary GH secretion is highly pulsatile in adult male rats and mice, where strong plasma peaks of GH are followed by periods when GH levels are below detection, whereas GH secretion is more frequent in females, resulting in a more continuous exposure to circulating GH. These sexually dimorphic plasma GH patterns stimulate sex differential patterns of tyrosine phosphorylation/activation and nuclear translocation of the transcription factors STAT5a and STAT5b (collectively, STAT5) (50). Thus, STAT5 activation is persistent in female liver but is intermittent in male liver, where it coincides with the onset of each plasma GH pulse (4, 43, 54). STAT5 positively regulates ~90% of male-biased genes and negatively regulates ~60% of female-biased genes in male mouse liver (5). STAT5 binding sites are found near 35 to 40% of sex-specific genes, suggesting they are directly regulated by STAT5 (54). However, a majority of sex-specific genes do not respond rapidly to GH-activated STAT5, suggesting indirect regulatory mechanisms (47, 48). Continuous GH infusion in male mice (i.e., a female-like GH pattern) abolishes the endogenous, pulsatile plasma GH pattern and downregulates male-biased genes while upregulating female-biased genes; however, many of these gene responses are slow, requiring several days (12). Moreover, precocious activation of STAT5 in prepubertal male rats does not induce an adult male-biased pattern of gene expression in the liver, indicating a requirement for additional factors to achieve sex-specific liver gene expression (4). Furthermore, the high sex specificity exhibited by some sex-biased genes (>500-fold differences in transcript levels between sexes) indicates tight regulation, suggesting a need for transcriptional repressors as well as transcriptional activators to maintain robust sex differences in the liver.

Several novel sex-biased transcription factors that may contribute to sex differences in the liver have been identified (47, 48). One factor, the transcriptional repressor BCL6, shows a 14-fold male bias in expression in rat liver, where it responds rapidly to GH (33). STAT5 binds to seven regions in the *Bcl6* gene (33, 46, 54), one of which has been associated with repression of *Bcl6* (46). BCL6 and STAT5 have distinct but overlapping DNA binding motifs, enabling them to bind DNA in a mutually exclusive manner; thus, BCL6 binding to *Socs2* is maximal between GH pulses, when STAT5 activity is minimal (3, 33). This interplay between STAT5 and BCL6 occurs on a genome-wide scale, with 52% of BCL6 binding sites overlapping a STAT5 binding site in male liver (54). Notably, binding sites shared by STAT5 and BCL6 are enriched for female-biased genes, supporting the proposal that BCL6 contributes to sex differences in the liver by preferentially repressing a subset of female-biased genes in males (54).

Two liver-enriched transcription factors, HNF6 and HNF3β, display a 2- to 3-fold female bias in their expression in rat liver (20, 52) and regulate the promoter of *CYP2C12*, a highly female-spe-

Received 29 June 2012 Returned for modification 26 July 2012
Accepted 31 August 2012
Published ahead of print 10 September 2012
Address correspondence to David J. Waxman, djw@bu.edu.
Supplemental material for this article may be found at http://mcb.asm.org/.

doi:10.1128/MCB.00886-12

cific gene (8). Furthermore, three female-specific liver transcription factors that are STAT5 dependent and GH regulated have been identified in mouse liver (23). One of these factors, CUX2, is expressed in a highly female-specific manner (female/male ratio, ~100:1) in livers of both rats and mice. CUX2 expression is ablated in adult female rat liver by hypophysectomy and can be induced in male liver to a normal female-like level by continuous GH infusion (23). CUX2 contains three Cut repeats and one homeodomain and displays a DNA binding specificity similar to that of the related protein CUX1 (15), but it exhibits more rapid DNA binding kinetics (10). Similar to CUX1, CUX2 can repress the $p21^{WAF1/CIP1/SDI1}$ promoter, but unlike CUX1, CUX2 does not activate the DNA polymerase α promoter (10). Moreover, in neural tissue, CUX2 regulates dendritic branching and spine formation by directly repressing *Xlr4b* (7).

Computational analyses using a CUX1 motif as an indicator of CUX1/CUX2 DNA binding (10) revealed a statistically significant overrepresentation of CUX binding sites in the promoter regions of male-biased genes that are positively regulated by STAT5 (23). In addition, an HNF6/CUX family motif is significantly enriched in the vicinity of STAT5 sites that display stronger binding in male than in female liver and is depleted near STAT5 sites that show stronger binding in female liver, as determined by global chromatin immunoprecipitation studies (ChIP-Seq) (54). Together, these findings suggest that a CUX-related factor, perhaps CUX2, represses STAT5-dependent male-biased genes in female liver. In the present study, we investigated this hypothesis by identifying CUX2-regulated genes using a combination of CUX2 overexpression in male mouse liver, CUX2 knockdown in female mouse liver, and ChIP-Seq to identify CUX2 binding sites and target genes on a genome-wide scale.

MATERIALS AND METHODS

Animals. All animal studies were carried out using protocols approved by the Boston University Institutional Animal Care and Use Committee. For the CUX2 overexpression study, 7-week-old male and female ICR-scid mice (Fox Chase ICR-scid mice; Taconic Farms, Inc., Hudson, NY) were injected via the tail vein with 1×10^9 PFU of adenovirus expressing bacterial β-galactosidase (adeno-βGal) combined with either 9×10^9 PFU or 5×10^8 PFU of adenovirus expressing CUX2 (adeno-CUX2), as specified. An empty adenovirus (adeno-CMV) was used as a control. Mice were killed at 3 or 5 days postinjection ($n = 7$ to 13 mice/sex/treatment group), and livers were snap-frozen in liquid nitrogen and stored at −80°C. The CUX2 knockdown study used 8-week-old female ICR mice (jax:CD-1 mice; Jackson Laboratory, Bar Harbor, ME). Mice were administered CUX2 small interfering RNA (siRNA) or control siRNA (nonspecific [luciferase] siRNA sequence) formulated in lipid C12-200 (26) or phosphate-buffered saline (PBS) (see below) at 1 mg/kg by tail vein injection. The impact of CUX2 siRNA on liver gene expression was assessed in mice killed at either 5 or 8 days postinjection ($n = 4$ to 13 mice/treatment group); the extent of liver CUX2 RNA knockdown was determined in female mice compared to mice administered control siRNA at 1 day postinjection. Livers were snap-frozen in liquid nitrogen and stored at −80°C. The CUX2 ChIP-Seq study used 7-week-old male and female ICR mice (crl:CD1 mice; Charles River Laboratories, Wilmington, MA).

EMSA. Cytoplasmic and nuclear extracts from 293T cells infected with adeno-CUX2 or transfected with a CUX2 plasmid or a control plasmid (16 μg plasmid per 10-cm tissue culture plate) were isolated using a NucBuster protein extraction kit (Novagen, Gibbstown, NJ). Electrophoretic mobility shift assay (EMSA) was performed using 30 μg of cytoplasmic or nuclear extract, 2 μl EMSA buffer (20% glycerol, 5 mM $MgCl_2$, 2.5 mM EDTA, 2.5 mM dithiothreitol, 250 mM NaCl, 50 mM Tris Cl, pH 7.5), and 1 μl containing 2 μg of poly(dI-dC) (Sigma-Aldrich Corp., St. Louis, MO) for a total volume of 14 μl. After incubation at room temperature for 10 min, a double-stranded ^{32}P-labeled oligonucleotide probe (1 μl, 10 fmol) was added, followed by incubation for 20 min at room temperature. Loading dye (2 μl of 30% glycerol, 0.25% bromophenol blue, and 0.25% xylene cyanol) was added, and the mixture was electrophoresed for 3 to 4 h at 100 to 130 V through a nondenaturing acrylamide gel (5.5% acrylamide and 0.07% bisacrylamide; National Diagnostics, Atlanta, GA) that was run in 0.5× TBE (44.5 mM Tris Cl [pH 8], 44.5 mM boric acid, 5 mM EDTA) and was preelectrophoresed at 4°C for 30 min at 100 V. Gels were dried and exposed to phosphorimager screens for 1 to 3 days, followed by analysis on a Typhoon Trio variable-mode imager (GE Healthcare, Piscataway, NJ). ImageQuant software was used to quantify gel bands. The CUX EMSA probe is 5′-TCGAGACGATATCGATAAGCTTCTTTTC-3′ (sense strand) (10). The antisense strand was end labeled with ^{32}P using T4 polynucleotide kinase, annealed to the sense strand, and purified on a BioSpin30 chromatography column (Bio-Rad Laboratories Inc., Hercules, CA).

RNA analysis. Total RNA was isolated from frozen individual livers using TRIzol reagent (Invitrogen, Carlsbad, CA). RNA was converted to cDNA using a high-capacity cDNA reverse transcription kit (Applied Biosystems, Foster City, CA). For the adeno-CUX2 study, triplicate 5-μl real-time quantitative PCR (qPCR) mixtures, each containing Power SYBR green PCR master mix (Applied Biosystems), 312 nM each qPCR primer, and 0.5 to 1.5 μl cDNA template, were loaded onto a 384-well plate and run through 40 cycles on an ABS 7900HT sequence detection system (Applied Biosystems). Data are graphed as relative values, normalized to the 18S rRNA content of each sample. For the CUX2 siRNA study, CUX2 RNA was quantified using a CUX2-specific Q2 probe and a QuantiGene 2.0 bDNA kit (Affymetrix, Inc., Santa Clara, CA), with the data graphed as relative values, normalized to the GAPDH (glyceraldehyde-3-phosphate dehydrogenase) RNA content of each sample. Statistical analysis of qPCR data was carried out by one-way analysis of variance (ANOVA) using PRISM software version 4 (GraphPad Software, Inc., La Jolla, CA). qPCR primers are listed in Table S1 in the supplemental material. RNA integrity (RIN number of ≥8.0) was determined using an Agilent Bioanalyzer 2100 (Agilent Technologies, Inc., Santa Clara, CA).

Adenovirus construction, amplification, and purification. The CUX2 cDNA cloned into plasmid pMX139/Myc/HA (10) was obtained from A. Nepveu, McGill University, and used for adenovirus construction. Cloning into an adenoviral expression vector (cytomegalovirus [CMV] promoter-internal ribosome entry site [IRES]-green fluorescent protein [GFP]) and subsequent generation of adenovirus (adeno-CUX2) were carried out by Welgen, Inc. (Worcester, MA). An empty adenovirus containing a CMV promoter-IRES-GFP cassette (adeno-CMV; Welgen, Inc.) was used as a control. Adenoviral stocks were propagated in human kidney 293A cells grown in 100-mm tissue culture plates at 37°C in a humidified 5% CO_2 atmosphere in Dulbecco modified Eagle medium (DMEM) containing 10% fetal bovine serum (FBS). Cells grown to ~90% confluence were infected with adeno-CUX2 or adeno-CMV at a multiplicity of infection of ~5 viral particles per cell. Alternatively, 3 to 5 ml of −80°C frozen culture supernatant obtained from adeno-CUX2- or adeno-CMV-infected 293A cells was used to infect a plate of 293A cells. At 2 or 3 days after infection, when ~80 to 90% of the cells were rounded and ~10 to 20% of cells were floating, the cells were harvested by centrifugation and the pellet was resuspended in 10 to 20 ml of buffer A (10 mM Tris Cl [pH 8.0], 1 mM $MgCl_2$). Virus was released from the cells by three freeze-thaw cycles, alternating between a −80°C freezer and a 37°C water bath, and the cell lysate was centrifuged at 4°C for 10 min at 3,000 rpm in a Sorvall RT 6000D centrifuge using an H1000B rotor. The supernatant was placed on ice, and the remaining cell pellet was reextracted in the same manner with 10 ml of buffer A. The supernatants were combined, treated with fresh Benzonase (0.5 to 1 unit/ml) at room temperature for 30 min, and then loaded on top of a CsCl step gradient comprised of 10 ml of light CsCl (1.2 g/ml; 22.39 g CsCl plus 77.6 ml of 10 mM Tris Cl, pH 8.0)

layered on top of 10 ml of heavy CsCl (1.45 g/ml; 42.23 g CsCl plus 57.77 ml of 10 mM Tris Cl, pH 8.0). Samples were centrifuged in a Sorvall Pro ultracentrifuge in an SW28 rotor at 4°C for 2 h at 20,000 rpm. The banded virus was collected, diluted with an equal volume of 10 mM Tris Cl (pH 8.0), and loaded on top of a second CsCl step gradient consisting of 4 ml each of light CsCl and heavy CsCl as described above. Samples were centrifuged in a Sorvall Pro ultracentrifuge in a SW41 Ti rotor at 4°C overnight at 20,000 rpm. The purified virus was desalted by dialysis against 10 mM Tris Cl (pH 8.0)–1 mM $MgCl_2$–10% glycerol. The virus titer was determined using an adeno-X rapid titer kit (Clontech Laboratories Inc., Mountain View, CA) and stored in aliquots at −80°C.

CUX2 siRNA design, synthesis, and formulation. A total of 24 siRNA duplexes were designed to target mouse CUX2 mRNA (NM_007804.2). All possible 19-mer oligonucleotide sequences derived from NM_007804.2, both sense and antisense, were aligned to the mouse RefSeq transcriptome using the FASTA34 software suite (http://fasta.bioch.virginia.edu). Oligonucleotide matches to off-target transcripts were tallied and scored according to the number and location of mismatches to off-target transcripts using a custom Perl script. Briefly, the algorithm weighs mismatches according to their position in the siRNA seed region, cleavage site, and remaining sites (with decreasing weights to the seed, cleavage, and remaining sites, respectively). Candidate duplexes (pairs of complementary sense and antisense 19-mers) were selected to maximize mismatches to off-target transcripts and avoid repeats ≥4 nucleotides (nt) long. Duplexes were further selected for predicted efficacy by choosing sequences that maximize thermal asymmetry and minimize GC content in the antisense seed region.

The luciferase-specific siRNA was that described earlier (42). Single-stranded chemically modified RNAs were synthesized at Alnylam Pharmaceuticals (Cambridge, MA) using solid-supported oligonucleotide methodology and standard phosphoramidite chemistry. All single strands were 21-mers and chemically modified at selected sites with either 2′-*O*-methyluridine or 2′-*O*-methylcytosine. Other nucleotides within the CUX2 siRNA sequence were unmodified ribonucleotides and contained a two-nucleotide deoxythymidine overhang at the 3′ end with a phosphorothioate backbone. The single strands were synthesized at a 0.2-μmol scale in 96-well plates on a MerMade192 DNA/RNA synthesizer (Bio-Automation, Inc., Irving, TX). The 2′-*O*-methyl and riboamidites were prepared at a 0.1 M concentration using ethyl thiotetrazole (0.6 M in acetonitrile) as an activator. The synthesized sequences were cleaved and deprotected in 96-well plates, using methylamine in the first step and fluoride reagent in the second step. The crude sequences were precipitated using acetone-ethanol at −20°C for 2 h. Following centrifugation and decanting of the solvents, the pellet was isolated and resuspended in 0.2 M sodium acetate buffer. The single strands were analyzed by liquid chromatography-mass spectrometry (LC-MS) to confirm their identity, by UV for quantification, and by IEX chromatography to determine purity. CUX2 single strands were precipitated and then purified on an AKTA purifier system (GE Healthcare) using a Sephadex G25 column run at ambient temperature. Sample injection and collection were performed in 96-well (1.8-ml-deep-well) plates. A single peak corresponding to the full-length sequence was collected in the eluent. The desalted CUX2 sequences were analyzed for concentration (A_{260}) and purity (by ion-exchange high-pressure liquid chromatography [HPLC]). The complementary single strands were then combined at a 1:1 molar ratio to form siRNA duplexes. The duplexes were formulated with RNAimax (Invitrogen Inc.) and prepared according to the manufacturer's protocol. The CUX2 siRNA duplexes were screened at two concentrations in primary mouse hepatocytes isolated as previously described (41). Dose-response curves were generated for the top-performing duplexes that gave 50% inhibitory concentrations (IC_{50}s) of <10 nM. Large-scale synthesis and *in vivo* testing in mice were carried out with the top CUX2 siRNA duplex (chr5: 122318587 to 122318605 [mm9]; sense strand, GuAGcGuGAGuGAcAu Gcu-dTs-dT, where lowercase u and c indicate 2′-O-methylated uridine and cytidine, respectively, dTs indicates 2′-deoxythymidine-3′-phosphorothioate, and dT indicates 2′-deoxythymidine-3′-phosphate).

Lipid nanoparticle (LNP) siRNA formulations were prepared using the lipid C12-200 (26). C12-200, along with the colipids distearoyl phosphatidylcholine, cholesterol, and methoxyl-polyethylene glycol 2000 (mPEG 2000)–dimyristoylglycerol (DMG) (1), was formulated with siRNA using a spontaneous vesicle formation formulation procedure (26). The LNPs had a C12-200/distearoyl phosphatidylcholine/cholesterol/PEG-DMG component molar ratio of ~50:10:38.5:1.5 at a final lipid/siRNA weight ratio of 7:1. The LNP siRNA formulations had a mean particle diameters of ~80 nm with >83% lipid entrapment efficiency, as determined using a modified Ribogreen assay (Invitrogen Inc.) (1).

Microarray design and statistical analysis. For the adeno-CUX2 study, liver RNA pools were prepared from two independent randomized sets of biological replicates ($n = 3$ to 7 mouse liver RNAs/pool) and used in two-color hybridization experiments in a loop design: (i) untreated male versus untreated female, (ii) adeno-CUX2-injected male (5 days) versus adeno-CMV-injected male (5 days), (iii) adeno-CUX2-injected female (5 days) versus adeno-CMV-injected female (5 days), and (iv) adeno-CUX2-injected male (3 days) versus adeno-CMV-injected male (3 days). For the CUX2 siRNA study, liver RNA pools were prepared from two independent randomized pairs of biological replicates ($n = 2$ to 7 mouse liver RNAs/pool) and used in two-color hybridization experiments in a loop design: (i) CUX2 siRNA-treated female (5 days) versus control siRNA-treated female and (ii) CUX2 siRNA-injected female (8 days) versus control siRNA-treated female. Biological replicates were analyzed as dye swaps to correct for dye bias, giving a total of 8 and 4 microarrays for the adeno-CUX2 study and the CUX2 siRNA study, respectively. Hybridization of fluorescence-labeled RNA to 41,174-feature Agilent microarrays was carried out for each pair of independent biological replicates. A Whole Mouse Genome oligonucleotide microarray kit 4 × 44K (catalog no. G4122F-014868 from Agilent Technology; GEO platforms GPL4134 and GPL7202) was used for both studies. Labeling, hybridization, scanning, and initial microarray analysis were conducted at the microarray core facility at Wayne State University (Detroit, MI).

Linear and LOWESS normalization were performed for each microarray using Agilent Feature Extraction software. The variation of pixel intensity for each feature (spot) on the array was input to the Rosetta error model, which was used for analysis of statistical significance of differential gene expression. The Rosetta error model provides a gene-specific estimate of error by incorporating two elements: a technology-specific estimate of error and an error estimate derived from replicate arrays (51). The technology-specific component utilizes an intensity-dependent model of error derived from numerous self-self hybridizations. Two arrays, based on independent pools of biological replicates, were used for each comparison of interest. By including the technology-specific estimate, the Rosetta error model avoids false positives that occur from underestimation of error when a small number of replicate arrays are available, giving an increase in statistical power equivalent to that which would be obtained with at least one additional replicate. For two-color microarrays, a log ratio error estimate is derived in the Rosetta error model from the individual error estimates of each sample (color) used in the cohybridization. Then, for each feature, an average log ratio and associated *P* value are obtained from replicate measurements (arrays) using the Rosetta error model error-weighted averaging method. In this approach, the average ratio is calculated by weighting the ratio from each sample inversely proportional to the variance of that sample. This produces an averaged ratio with the smallest possible error. Validation with spike-in experiments has demonstrated that the Rosetta error model has superior accuracy in detecting and quantifying relative gene expression compared to other statistical methods commonly used in microarray analysis (39). All microarray and ChIP-Seq genomic coordinates reported in this study are based on mouse genome release mm9.

The statistical significance of differential expression of each gene was determined by application of a filter ($P < 0.0001$, unless indicated other-

wise) to the Rosetta-generated *P* values. The number of microarray probes expected to meet the significance threshold of $P < 0.0001$ by chance is $0.0001 \times 41{,}174$ probes or 4.1 probes. The actual number of probes that met this *P* value ranged from 1,662 (untreated male versus untreated female) to 3,390 (adeno-CUX2 male versus adeno-CMV male at 5 days) in the adeno-CUX2 study (false-discovery rate ranging from 0.25% [4/1,662] to 0.12% [4/3,390]) and from 4,715 (CUX2 siRNA female [8 days] versus control siRNA female) to 5,170 (CUX2 siRNA female [5 days] versus control siRNA female) in the CUX2 siRNA study (false-discovery rates of 0.085% [4/4,715] and 0.077% [4/5,170], respectively). Probes whose raw signal was not >99% of the background population signal did not pass Agilent's "well-above-background" specification and were removed (137 and 189 probes in the adeno-CUX2 and CUX2 siRNA studies, respectively). Finally, a |fold change| filter of >1.5-fold was combined with the $P < 0.0001$ filter to limit consideration to genes showing expression ratios of >1.5 (upregulated genes) or <0.667 (downregulated genes). When two or more probes assigned the same gene name gave the same pattern of regulation across the microarray set being compared, i.e., redundant probes (as indicated by assignment to the same total flag sum [TFS] group [see Table S2 in the supplemental material and below]), only the probe with the lowest set of *P* values was retained. Probes associated with the same gene name but different TFS groups were retained. After removing redundant probes, 5,244 and 4,706 probes (genes) met the above specific *P* value, expression ratio, and well-above-background filters for the adeno-CUX2 study (array comparisons 1 to 3) and the CUX2 siRNA study, respectively. Of the 5,244 regulated genes in the adeno-CUX2 study, 1,662 genes showed significant sex differences (male versus female |fold change| of >1.5 and $P < 0.0001$) and were designated sex biased (sex-specific genes), 1,257 genes were classified as stringent sex-independent genes (male versus female |fold change| of <1.2, $P > 0.01$, and Agilent microarray signal intensity of ≥25), and 2,325 other genes showed sex-independent expression only under nonstringent conditions (male versus female |fold change| of between 1.2 and 1.5 [inclusive] and $0.0001 \leq P \leq 0.01$) (see Table S2 in the supplemental material). Of the 4,706 regulated genes in the CUX2 siRNA study, 599 genes showed significant sex differences (using the thresholds and filters described above) and were designated sex-biased (sex-specific) genes, 1,622 genes were classified as stringent sex-independent genes, and 2,485 other genes showed sex-independent expression only under nonstringent conditions based on their expression profiles in untreated CD-1 mouse livers, as determined previously (47) using the same microarray platform (see Table S3 in the supplemental material).

Microarray data analysis. A system of binary and decimal TFS flags (5) was used to classify the regulated genes in each microarray study based on expression ratios and *P* values across microarray comparisons (see Tables S2 and S3 in the supplemental material). Hierarchical clustering of $\log_2$ gene expression ratios and heat map generation were carried out separately for the sex-biased genes and stringent sex-independent genes using Cluster (9) and Java TreeView (40). The DAVID annotation tool (13, 14) was used to analyze genes in hierarchical clusters to identify enrichment clusters deemed significant (minimum enrichment score [ES] of 1.3, which is equivalent to an uncorrected *P* value of 0.05). Enrichment of genes altered by CUX2 overexpression in mouse liver in gene sets that showed a development change from 3 to 8 weeks in a previous microarray study (6) was calculated using genes common to both microarray platforms (G4846A-026655 used in the developmental study [6] and G4122F-014868 used in the present adeno-CUX2 study). For sex-biased genes, only genes that showed sex bias in both studies were used when calculating the enrichment score. Comparisons of sex-independent genes utilized the set of 1,257 stringent sex-independent genes (defined above) to exclude genes showing a weak sex bias in expression and genes that gave low microarray signal intensities. Enrichment *P* values for all comparisons were calculated using the two-tailed Fisher exact test, with a *P* value of <0.0001 deemed significant.

CUX2 antibody production and purification. A plasmid encoding glutathione *S*-transferase (GST) fused to mouse CUX2 protein amino acids 356 to 415 (CUX2-356) was obtained from A. Nepveu, McGill University, who had previously used this construct to produce a CUX2-specific antibody that is not cross-reactive with CUX1 (10). GST–CUX2-356 plasmid transformation into competent *Escherichia coli* cells was followed by the inoculation of a bacterial culture grown in LB medium with ampicillin and the addition of isopropyl-β-D-1-thiogalactopyranoside at a concentration of 0.1 mM for a 3-h incubation at 37°C to induce protein expression. Cells were centrifuged, washed with 1× PBS, and then sonicated while on ice. Lysed cells were centrifuged, and the supernatant was passed through a column of glutathione-agarose beads (Sigma-Aldrich Corp) and then washed with 1× PBS. The beads were then treated with 50 mM Tris Cl (pH 8.0) to elute the GST–CUX2-356 protein. Inoculation of New Zealand White rabbits with purified GST–CUX2-356 protein (200-μg initial injection, followed by injection of 100 μg after 2 weeks, 4 weeks, and 6 weeks) and serum collection were performed by ProSci, Inc. (Poway, CA). GST and GST–CUX2-356 fusion protein columns were prepared by incubating glutathione-agarose beads with supernatant from *E. coli* cells expressing either GST or GST–CUX2-356 (as described above) and with the cross-linking chemical dimethylpimelimidate (0.12 g in 20 ml of 0.2 M borate buffer, pH 9.0). Affinity purification of the CUX2-356 antibody was performed by passing the serum through a GST column three times as described previously (10) and then passing the flowthrough over a GST–CUX2-356 affinity column and eluting the antibody with 0.2 M glycine-HCl (pH 2.5). The eluted antibody was then dialyzed at 4°C against a solution of PBS-glycerol (1:1, vol/vol), and aliquots were stored at −80°C.

Chromatin cross-linking and DNA fragmentation. Fresh liver tissue from ICR mice (crl:CD1; Charles River Laboratories) was homogenized on ice in homogenization buffer (10 mM HEPES [pH 7.6], 25 mM KCl, 0.15 mM spermine, 0.5 mM spermidine, 1 mM EDTA, 2 M sucrose, and 10% glycerol) with Complete protease inhibitor cocktail (1 tablet/25 ml) (Santa Cruz Biotechnology, Inc., Santa Cruz, CA). The homogenate was loaded onto a 3-ml cushion of homogenization buffer and centrifuged in a Sorvall Pro ultracentrifuge in an SW41 Ti rotor at 4°C at 25,000 rpm for 30 min. The pelleted nuclei from each liver were resuspended in 2.5 ml of cross-linking buffer (10 mM HEPES [pH 7.6], 25 mM KCl, 0.34 M sucrose, 0.15 mM 2-mercaptoethanol, 2 mM $MgCl_2$) and incubated with 1% formaldehyde (final concentration) for 9 min in a 30°C water bath with periodic shaking. Cross-linking was halted by addition of a 1.25 M glycine (pH 8.0) solution (final concentration, 0.125 M), followed by incubation for 5 min at room temperature. Samples were placed on ice, layered on a 3-ml cushion of homogenization buffer, and centrifuged at 4°C at 25,000 rpm for 30 min. The cross-linked nuclear pellet was resuspended in 2.4 ml of 1× radioimmunoprecipitation assay (RIPA) buffer (50 mM Tris Cl [pH 8.1], 150 mM NaCl, 1% Igepal CA-630, 0.5% sodium deoxycholate) containing 0.5% SDS and Complete protease inhibitor cocktail and sonicated using a Branson Sonifier 250D with a tapered microtip at 35% power output for 15 s on and 45 s off, for a total on time of 6 min (24 cycles). A 15-μl aliquot of the sonicated chromatin was reverse cross-linked, treated with RNase A and proteinase K, and electrophoresed on a 1% agarose gel to size the fragments. The majority of DNA fragments ranged from 100 to 400 bp. The remaining sonicated chromatin was snap-frozen in liquid nitrogen and stored at −80°C.

ChIP. All steps were performed at 4°C, unless indicated otherwise, using sonicated cross-linked chromatin. Protein A Dynal magnetic beads (Invitrogen Corporation, Carlsbad, CA) were washed with blocking solution (1× PBS containing 1% bovine serum albumin) and then incubated overnight at 4°C on a rocker with 100 μg purified CUX2-356 antibody diluted in blocking solution per 45 μl beads. Beads were washed three times with blocking solution and incubated overnight at 4°C with 150 μg of sonicated chromatin diluted 5-fold with 1× RIPA buffer containing Complete protease inhibitor tablet and without SDS. Two 50-μl input DNA samples taken from the diluted chromatin sample were reverse

cross-linked, treated with RNase A and proteinase K, extracted with phenol-chloroform-isoamyl alcohol, and used for qPCR analysis. The beads from the chromatin immunoprecipitation (ChIP) sample were washed twice with 1× RIPA buffer containing 0.1% SDS, three times with 1× RIPA buffer containing 0.1% SDS and 0.5 M NaCl, and then once with TE buffer (10 mM Tris Cl [pH 8], 1 mM EDTA). Elution buffer (50 mM Tris Cl [pH 8.1], 10 mM EDTA, 1% SDS) was added to the beads, which were incubated in a 65°C water bath for 30 min with periodic vortexing. The eluted ChIP samples were purified using the QIAquick gel extraction kit (Qiagen, Valencia, CA) and used for real-time PCR analysis.

High-throughput sequencing and ChIP-Seq analysis. CUX2 ChIP-Seq data were obtained from each of 3 independent sets (i.e., biological replicates) of adult female mouse liver (18.4 million mapped reads) and from 2 independent biological replicates of adult male mouse liver (8 million mapped reads). DNA isolated by ChIP using anti-CUX2 antibody was prepared for sequencing using an SPRI-TE nucleic acid extractor (Beckman Coulter Genomics, Danvers, MA) followed by PCR enrichment with bar coding. The SPRI-TE instrument automates end repair, A addition, Illumina adapter ligation, and size selection (200 to 400 nt). Sample preparation and 35-nt, single-end read sequencing on an GAII instrument (Illumina, San Diego, CA) were carried out at the BioMicro Center at MIT (Cambridge, MA). Raw sequencing data for individual mouse livers were analyzed to ensure quality control and then combined for each sex, to give one combined adult male and one combined adult female CUX2 ChIP-Seq data set. MACS software (55) with default parameters was used to identify 1,471 significant CUX2 peaks (CUX2 binding sites) ($P < 1E-6$; i.e., MACS score of >60) based on CUX2 binding in adult female liver compared to adult male liver, where little or no CUX2 is present and which was therefore used as a background data set in the MACS analysis. For each ChIP-Seq peak, the nearest gene within 10 kb of the peak region was defined as the peak target. The Flexmodule_motif from the CisGenome package (17) was used for *de novo* motif discovery with default parameters. Motif position weight matrices were mapped to genomic coordinates using motifmap_matrixscan_genome implemented in CisGenome with default parameters. Sequence logos for *de novo*-identified motifs were generated using STAMP (30), which was also used to compare *de novo*-identified motifs with TRANSFAC matrices. Enrichment was calculated by comparison to a set of randomly selected genomic regions as background (17) for each of 97 motif families (derived from TRANSFAC and JASPAR databases) (27) together with the CUX2 motif identified *de novo* using the female liver CUX2 peak set. Enrichment of the CUX2 binding site target genes in the set of genes whose expression is altered by adeno-CUX2 in male liver (5 days), adeno-CUX2 in female liver (5 days), or CUX2 siRNA treatment in female liver (5 and 8 days) (|fold change| of >1.5 and $P < 0.0001$) was calculated using RefSeq genes only. Enrichment *P* values were calculated using the two-tailed Fisher exact test, with a *P* value of <0.0001 deemed significant. ChIP-Seq and DNase hypersensitivity site (DHS) peak overlap analysis was based on a minimum of a 1-bp overlap between peak sets. Transcriptional regulators were identified by the Gene Ontology descriptors "DNA binding" and "transcription."

Microarray data accession numbers. Microarray data files are available at the Gene Expression Omnibus (GEO) website (http://www.ncbi.nlm.nih.gov/geo/) as GEO series GSE35897 (adeno-CUX2 study, samples GSM877189 to GSM877196) and GSE37078 (CUX2 siRNA study, samples GSM910318 to GSM910321). Microarray expression profile data for untreated CD-1 mouse livers determined previously (47) are available as GEO series GSE17644 (samples GSM440277 and GSM40278). Raw and mapped sequencing reads for CUX2 ChIP-Seq for male and female liver samples are available as GEO series GSE35985 (samples GSM878678 and GSM878679).

RESULTS

Overexpression of CUX2 in adult mouse liver. CUX2 is expressed at a ~100-fold-higher level in female than in male mouse liver (23). To identify genes regulated by CUX2, we used an adenoviral vector to overexpress CUX2 in male mouse liver. Adenovirus-induced liver gene expression was facilitated by using *scid* immunodeficient mice, which clear adenovirus slowly (34) and provide for transgene expression in a much higher fraction of hepatocytes than immunocompetent mice (Fig. 1A). Adeno-CUX2 yielded high levels of CUX2 immunoreactive protein compared to those in uninfected livers or livers infected with a control virus (adeno-CMV) (Fig. 1B). The expressed CUX2 protein localizes to the nucleus and binds specifically to a CUX DNA binding site oligonucleotide (EMSA) probe (Fig. 1C).

Adeno-CUX2 induced high levels of CUX2 RNA in both male and female liver after 5 days (Fig. 1D). In male liver infected with adeno-CUX2, female-biased genes were highly induced (Fig. 2A to C) and male-biased genes were repressed (Fig. 2D to G), while a control virus, adeno-CMV, had little or no effect. In female liver, where CUX2 is already expressed, adeno-CUX2 had limited effects on female-biased genes (a 2- to 3-fold increase in *Prom1* and a 4-fold decrease in *Cyp2b9*) (Fig. 2A and B). Further repression of the already low levels of several male-biased genes was also apparent (Fig. 2D, E, and G). Overexpression of CUX2 in male liver at a more modest level could be achieved by using a 20-fold-lower dose of adeno-CUX2; however, little or no change in expression was observed for any of the sex-biased genes examined (see Fig. S1 in the supplemental material). Thus, CUX2 overexpression is required to effect the observed changes in sex-dependent liver gene expression.

Genome-wide impact of CUX2 overexpression. The effects of CUX2 overexpression were evaluated by global gene expression analysis (Fig. 3A; see Fig. S2A in the supplemental material, and see Table S2 in the supplemental material for data on individual genes). Partial feminization of male liver was observed (Fig. 3A, lane 2 versus lane 1), with 35% of male-biased genes repressed and 36% of female-biased genes induced (Table 1). Very few male-biased genes were induced by CUX2 overexpression, and few female-biased genes were repressed. Many fewer sex-biased genes were affected by CUX2 overexpression in female liver, where there is already a substantial basal level of CUX2, but again, male-biased genes were primarily repressed and female-biased genes were primarily induced (Fig. 3A, lane 3; Table 1). The same general trends were seen when male mice were infected with adeno-CUX2 for a shorter time period (3 days) (see Fig. S3 in the supplemental material). Male-biased genes repressed by adeno-CUX2 in both male and female liver generally showed higher expression levels in female liver than male-biased genes repressed in male liver only (see Fig. S4 and Table S2 in the supplemental material). This suggests that the endogenous level of CUX2 in female liver is limiting with respect to its ability to fully repress the more highly expressed male-biased genes. CUX2 overexpression also altered the expression of stringent sex-independent genes, with more genes being upregulated than downregulated and with a very similar response pattern in both sexes (Table 1; see Fig. S2A [lane 2 versus lane 3] in the supplemental material).

Functional gene groups affected by CUX2 overexpression were identified by Gene Ontology analysis. Significant annotation clusters associated with both male-biased and female-biased genes affected by CUX2 include cytochrome P450/monooxygenase activity, transmembrane, and signal peptides. Male-biased genes were additionally associated with pheromone/odorant binding, GPCR/olfactory receptors, and muscle cell differentiation, while

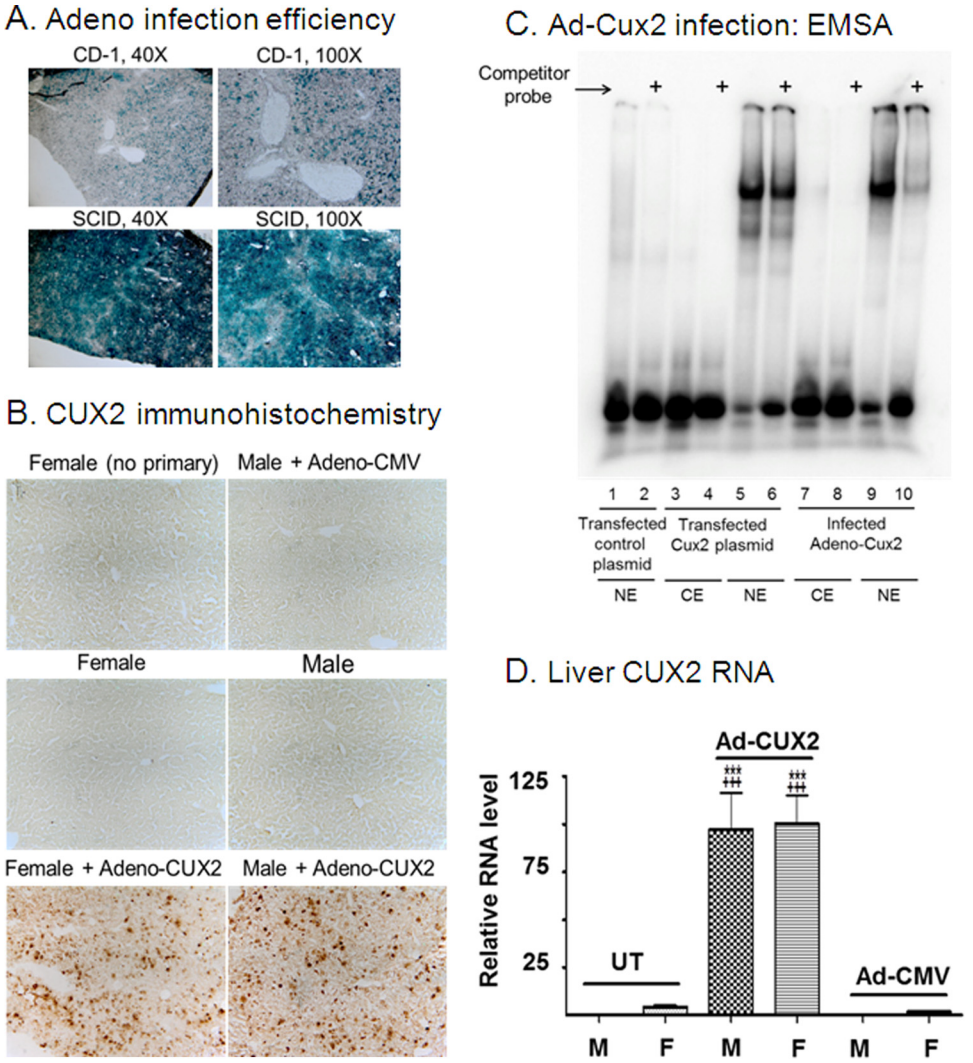

FIG 1 Adenoviral overexpression of CUX2. (A) Efficiency of adenoviral infection of livers in immunocompetent (CD-1) and immunodeficient (*scid*) mice. Shown are liver cryosections of CD-1 and *scid* mice infected with 1×10^9 PFU of adeno-βGal, killed 2 days later, and then stained with X-Gal (5-bromo-4-chloro-3-indolyl-β-D-galactopyranoside), at magnifications of ×40 and ×100. (B) Shown are cryosections prepared from male and female mouse livers that were untreated or treated with adeno-CUX2 or adeno-CMV (9×10^9 PFU) and killed 5 days later. Immunohistochemistry was carried out using either no primary antibody or with a CUX2-specific antibody (CUX2-356) at a 1:200 dilution. Magnification, ×200. (C) EMSA analysis of cytoplasmic extract (CE) or nuclear extract (NE) prepared from 293T cells transfected with either a control plasmid or a plasmid expressing CUX2 or from cells infected with adeno-CUX2; extracts were analyzed by EMSA using a ^{32}P-labeled CUX EMSA probe. A 10-fold excess of unlabeled probe was used as the competitor probe. (D) qPCR analysis of CUX2 RNA levels in livers from male (M) and female (F) mice that were untreated (UT) or treated with adeno-CUX2 or adeno-CMV and killed 5 days later. Relative RNA levels are shown, normalized to the 18S RNA of each sample, based on $n = 7$ to 13 individual livers/group (mean ± standard error of the mean [SEM]). Statistical analysis (one-way ANOVA with Bonferroni posttests) was as follows: ***, $P < 0.001$ for untreated versus adeno-CUX2; +++, $P < 0.001$ for adeno-CUX2 versus adeno-CMV.

female-biased genes contained significant annotation clusters relating to immune response, cell cycle/condensed chromosomes, and secreted proteins (see Table S4A in the supplemental material). Functional gene groups associated with other sets of genes that responded to adeno-CUX2 are presented in Tables S4B and C in the supplemental material.

CUX2 knockdown in female liver. The studies described above were complemented by investigation of the effects of CUX2 knockdown in female liver using a CUX2-specific short interfering RNA (CUX2 siRNA), which decreased CUX2 RNA levels by 80 to 90% (Fig. 4A). Global transcriptome analysis revealed a similar pattern of gene responses at both 5 days and 8 days after CUX2 siRNA treatment (Fig. 3B; see Fig. S2B in the supplemental material). The full data set is presented in Table S3 and summarized in Table S5 in the supplemental material, and functional gene groups affected by CUX2 siRNA are detailed in Table S6 in the supplemental material. Three times as many female-biased genes were repressed by CUX2 siRNA as were induced (Fig. 3B, clusters F and H; see Table S5 in the supplemental material). Conversely, twice as many male-biased genes (Fig. 3B, clusters G and I) were induced by CUX2 siRNA as were repressed (see Table S5 in the supplemental material) (based on gene responses at 8 days or genes showing the same response at 5 and 8 days after CUX2 siRNA). Overall, 1,035 genes responded in a reciprocal manner to

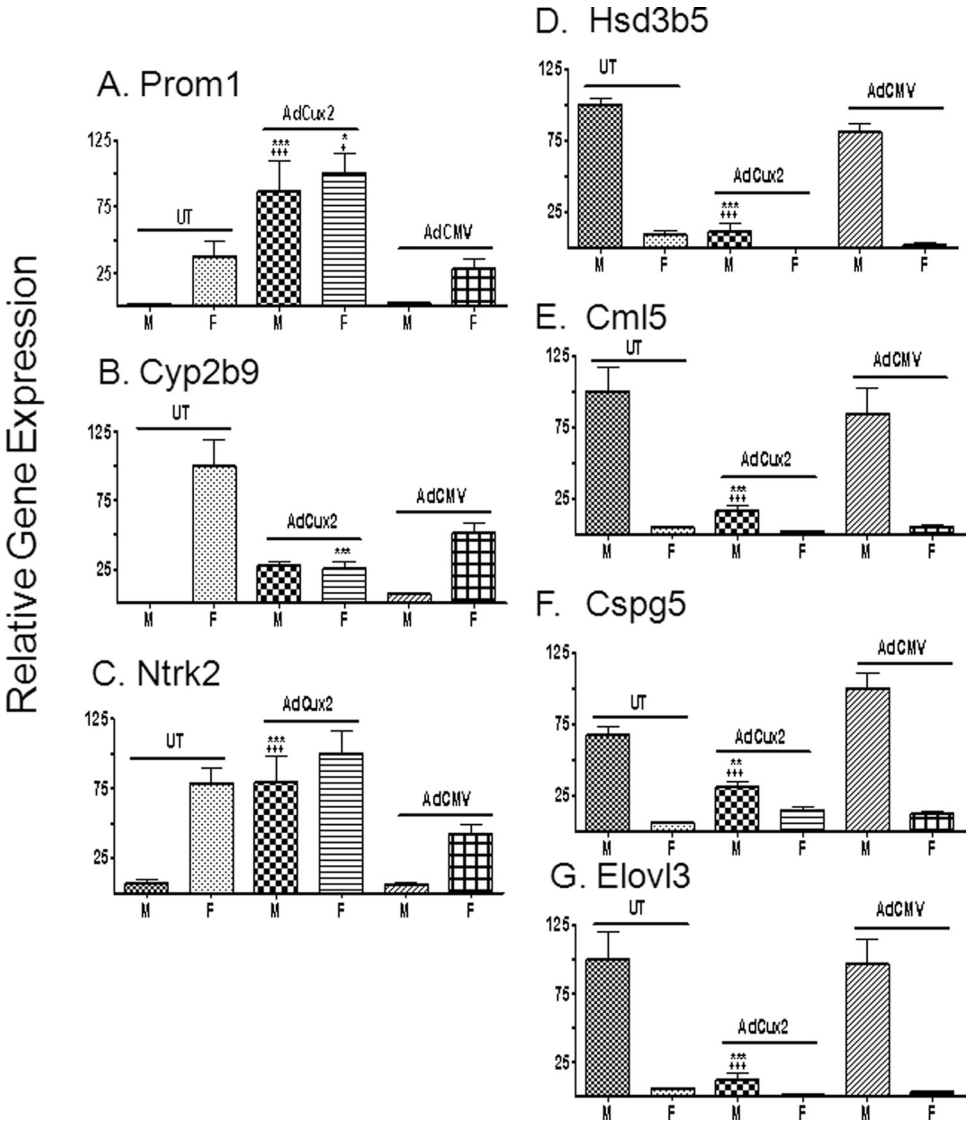

FIG 2 Effect of adeno-CUX2 on sex-biased liver gene expression. qPCR analysis of liver RNA levels from male (M) and female (F) mice that were untreated (UT) or treated with adeno-CUX2 or adeno-CMV and killed 5 days later is shown. Data shown for the 7 indicated sex-biased genes (female-biased genes [A to C] or male-biased genes [D to G]) are relative RNA levels, normalized to the 18S RNA of each sample, based on $n = 7$ to 13 individuals/group (mean ± SEM). Statistical analysis (one-way ANOVA with Bonferroni posttests) was as follows: *, $P < 0.05$; **, $P < 0.01$; ***, $P < 0.001$ for untreated versus adeno-CUX2; +, $P < 0.05$; ++, $P < 0.01$; +++, $P < 0.001$ for adeno-CUX2 versus adeno-CMV.

CUX2 siRNA treatment in female liver compared to adeno-CUX2 treatment in male liver (see Table S7 in the supplemental material). Moreover, the genes repressed by CUX2 siRNA in female liver at both 5 and 8 days were enriched for genes induced by adeno-CUX2 in male liver (ES = 3.74; $P = 3.48E-153$), and the genes induced by CUX2 siRNA at both time points were enriched for genes suppressed by adeno-CUX2 (ES = 3.95; $P = 6.23E-48$). Functional gene groups affected by adeno-CUX2 and CUX2 siRNAs in a reciprocal manner are presented in Table S8 in the supplemental material.

Liver CUX2 cistrome. CUX2 binding sites were identified in mouse liver by ChIP-Seq using an antibody raised to CUX2 amino acids 356 to 415 (10), which distinguishes CUX2 from the related CUX1 (see Fig. S5 in the supplemental material). A total of 1,471 CUX2 binding sites (CUX2 peaks) (see Table S9 in the supplemental material) were identified in female but not male mouse liver, where CUX2 protein is essentially undetectable (23), supporting the specificity of the CUX2 antibody. Eighty-one percent of the CUX2-bound regions overlapped a liver DNase I-hypersensitive site, i.e., an open chromatin region (25) (see Table S9A in the supplemental material). The frequency of overlap increased with increasing CUX2 peak score (Fig. 5A), reaching 86% when only the 718 strongest CUX2 peaks were considered (i.e., MACS score of >100) (see Table S9C in the supplemental material). CUX2 peaks were distributed 5% in promoters, 46% in introns, and 46% in intergenic regions (Fig. 5B).

A CUX2 binding motif with the consensus sequence (A/G)ATCAAT was identified by *de novo* motif discovery using the CUX2 ChIP-Seq peak set; this motif is most closely related to that of HNF6 (*E* value of $<10^{-9}$) and more distantly related to the motifs

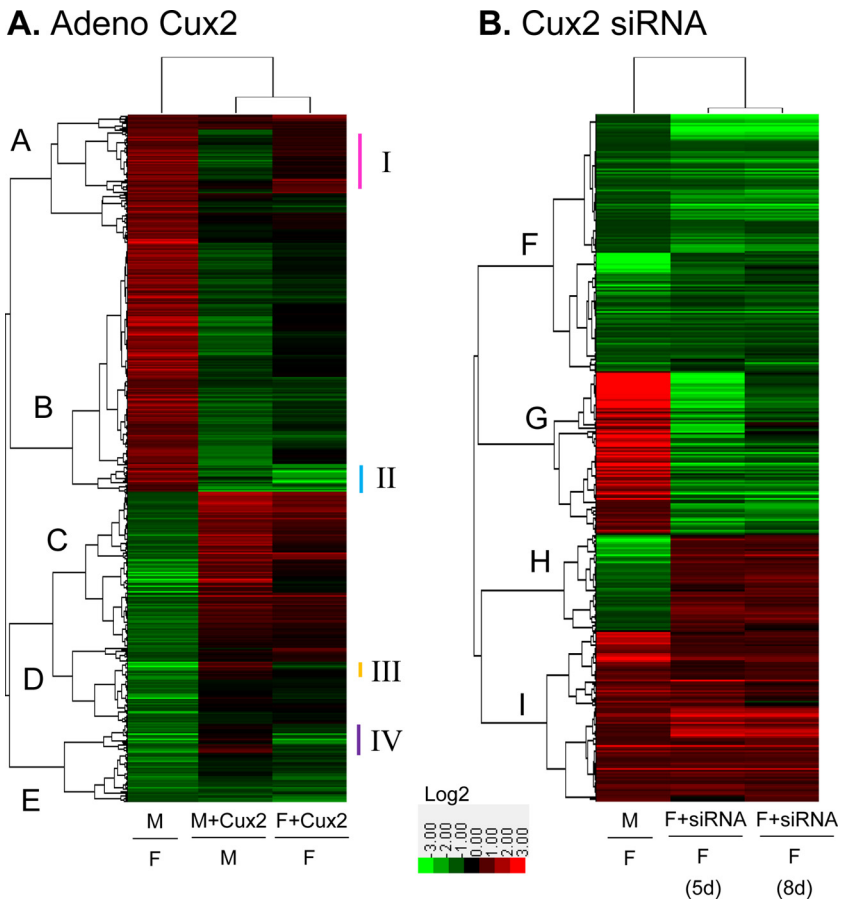

FIG 3 Heat maps displaying patterns of expression for sex-biased genes altered by adeno-CUX2 (A) and CUX2 siRNA (B). Genes are depicted based on their expression ratios across the three microarray comparisons indicated at the bottom of each heat map. Colors range from bright red (upregulation; $\log_2$ ratio, ≥ 3) to bright green (downregulation; $\log_2$ ratio, ≤ -3). Hierarchical clustering was performed based on Pearson's correlation of $\log_2$ ratios. The dendrograms at the top identify arrays showing the greatest similarity in their patterns of expression. M, untreated male liver; F, untreated female liver; M+CUX2 and F+CUX2, 5-day adeno-CUX2-treated male and female liver, which were, respectively, compared to adeno-CMV-treated male and female liver; F+siRNA, 5-day or 8-day CUX2 siRNA-treated female liver (as indicated) compared with nonspecific siRNA-treated female liver. (A) Male-biased gene clusters are labeled A and B, and female-biased clusters are labeled C to E. (B) Male-biased gene clusters are labeled G and I, and female-biased clusters are labeled F and H. Hierarchical clustering identified one cluster of male-biased genes that showed greater downregulation in female than in male liver (cluster II) and several clusters that displayed opposite responses in male and female liver (clusters I, III, and IV), marked on the right of panel A.

for PBX1 (10^{-5} to 10^{-7}) and CUX1/CDP (10^{-5} to 10^{-6}) (Fig. 5C). A second *de novo*-identified motif in the CUX2 peak set matched that of the PPAR/HNF4/COUP family (*E* value of $<10^{-16}$). Other *de novo*-identified motifs are shown in Fig. S6 in the supplemental material, together with their most closely related motifs in the TRANSFAC database. Consistent with these findings, motifs enriched in the CUX2 peak set include those describing the HNF6/CDP family (ES = 5.4), PBX1 (ES = 2.2), and the PPAR/HNF4/COUP family (ES = 1.8) (see Tables S9C and D in the supplemental material). The frequency of CUX2 motifs was highest in the strongest CUX2 peaks (highest MACS peak scores), but even the weakest CUX2 peaks showed a 50% occurrence of CUX2 motifs (Fig. 5D). Similar results were obtained for HNF6/CDP and PBX1 motifs (see Fig. S7A and B in the supplemental material), which may reflect the high frequency of overlap between these motifs and the CUX2 motif (~85% for HNF6/CDP and ~50% for PBX1 [see Fig. S7C in the supplemental material]). There was no consistent relationship between CUX2 peak strength and the occurrence of PPAR/HNF4/COUP family motifs in the CUX2 peak set (see Fig. S7D in the supplemental material).

Recently, we identified sex-enriched STAT5 binding sites in mouse liver chromatin that correlated well with sex-biased STAT5 target gene expression (54). The male-enriched and female-enriched STAT5 binding sites are both described by the same STAT5 motif; however, the male-enriched STAT5 peak regions are additionally associated with an HNF6/CDP family motif (54). Given our finding that CUX2 binding sites are best represented by an HNF6-related motif (Fig. 5C), we examined the association of sex-enriched STAT5 binding with CUX2 peaks. Notably, CUX2 binding sites in female liver were enriched at genomic regions where STAT5 binding is significantly higher in male than in female liver (Fig. 5E). An even greater enrichment was seen at those male-enriched STAT5 binding sites that overlap an HNF6/CDP motif (see Table S9A in the supplemental material), indicating that CUX2 has a propensity to bind in the vicinity of male-enriched STAT5 binding sites. Examples of CUX2 peaks overlapping a male-enriched STAT5 peak are shown in Fig. 6A, B, and F. Overall, ~40% of CUX2 ChIP-Seq peaks have peak summits within 500 bp of a STAT5 peak summit, indicating a close association between these two factors (Fig. 5F). Moreover, a significantly

TABLE 1 Impact of CUX2 overexpression in male and female mouse liver[a]

Gene category (total no. of genes)	Genes responding in male liver		Genes showing same response in female liver		Genes responding in female liver only	
	No.	%	No.	%	No.	%
Male biased (912)						
Induced by CUX2	16	1.8	10	1.1	27	3.0
Repressed by CUX2	320	35.1	70	7.7	14	1.5
Female biased (750)						
Induced by CUX2	273	36.4	103	13.7	13	1.7
Repressed by CUX2	38	5.1	24	3.2	49	6.5
Stringent sex independent (10,935)						
Induced by CUX2	607	5.6	370	3.4	142	1.3
Repressed by CUX2	290	2.7	119	1.1	220	2.0

[a] Liver RNA isolated from male and female mice infected with adeno-CUX2 for 5 days was analyzed by microarray in comparison to adeno-CMV (control)-infected liver RNA. Sex-biased and stringent sex-independent genes were determined by microarray analysis carried out using the same mouse strain used for these studies.

greater number of CUX2 peaks in female liver overlapped a male-enriched STAT5 peak (182 CUX2 peaks) than with a female-enriched STAT5 peak (15 CUX2 peaks) (P value for distribution significance = 7.16E−39) (see Table S9A in the supplemental material).

Sex-biased STAT5 binding is positively correlated with sex-differential chromatin accessibility, assayed by differential DNase hypersensitivity (54). Given the association of CUX2 binding sites with male-enriched STAT5 binding (Fig. 5E), we investigated the overlap of CUX2 peaks with male-biased DNase hypersensitivity sites. The most highly male-biased DNase-hypersensitive sites were ~7-fold more likely to be associated with a CUX2 peak in female liver than the most highly female-biased hypersensitive sites (Fig. 5G; see examples in Fig. 6A, B, and F). Overall, 143 CUX2 peaks overlapped a male-biased hypersensitive site, compared to only 19 CUX2 peaks that overlapped a female-biased hypersensitive site (P = 1.0E−10). Moreover, 90% of the CUX2-bound, male-biased DNase-hypersensitive sites showed decreased hypersensitivity in livers of male mice given a continuous infusion of GH for 7 days (female-like plasma GH pattern); i.e., chromatin accessibility at these sites is hormone responsive (see Table S9A in the supplemental material). Of note, a majority (68%) of the 143 genomic regions that are preferentially DNase hypersensitive in male liver and bind CUX2 in female liver are also DNase hypersensitive in female liver (see Table S9C in the supplemental material). Thus, while the corresponding chromatin regions are more accessible in male liver, they are nevertheless available for CUX2 binding in female liver. Finally, although CUX2 displays transcriptional repressor activity (10), no consistent relationship was seen between CUX2 MACS peak scores and the occurrence of the repressive chromatin mark H3-K27me3 (see Fig. S7E in the supplemental material).

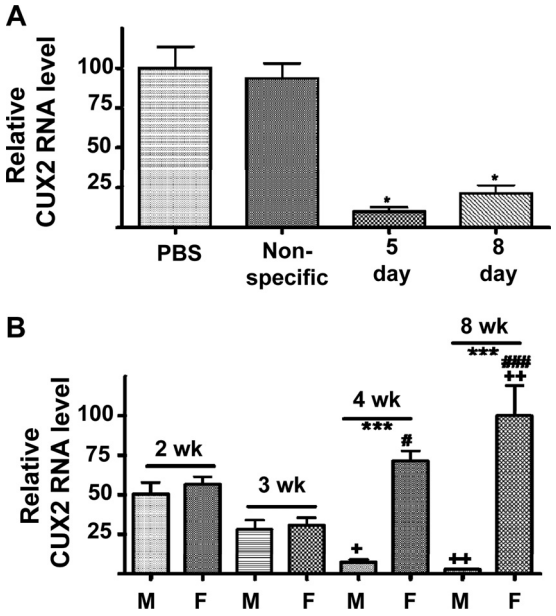

FIG 4 CUX2 RNA in mouse liver. (A) Impact of CUX2 siRNA. Quantigene 2.0 analysis of CUX2 RNA levels in livers of female mice treated with PBS, nonspecific siRNA, CUX2 siRNA (5 days), or CUX2 siRNA (8 days) is shown. Data shown are relative CUX2 RNA levels, normalized to the GAPDH RNA of each sample, based on n = 5 to 13 individuals per group (mean ± SEM). Statistical analysis (one-way ANOVA with Bonferroni posttests): *, $P < 0.05$. (B) Changes during postnatal development. qPCR analysis of relative RNA levels in male (M) and female (F) mouse liver at 2, 3, 4, and 8 weeks of age is shown. Data are normalized to the 18S RNA of each sample and based on n = 10 to 13 individuals per group (mean ± SEM). Statistical analysis (one-way ANOVA with Bonferroni posttests) was as follows: ***, $P < 0.001$ (for M versus F); +, $P < 0.05$; ++, $P < 0.01$ (for 2 weeks versus 4 or 8 weeks); #, $P < 0.05$; ###, $P < 0.001$ (for 3 weeks versus 4 or 8 weeks).

Relationship between CUX2 target genes and CUX2-dependent gene induction and gene repression. The above findings suggest that CUX2 enforces liver sex differences by preferentially repressing gene expression in female liver by binding near male-biased genes; in contrast, in male liver, chromatin at these CUX2 binding sites is more open and exhibits greater occupancy by STAT5. Supporting the proposal that CUX2's mechanism of action involves direct repression, genes located within 10 kb of a CUX2 binding site (putative CUX2 target genes [see Table S9C in the supplemental material]) are significantly enriched in the set of genes repressed following adeno-CUX2 infection. In contrast, CUX2 target genes are significantly depleted in the set of genes induced upon adeno-CUX2 infection. Moreover, the putative CUX2 target genes are enriched in the set of genes induced by CUX2 siRNA but not in the set repressed by CUX2 siRNA (see

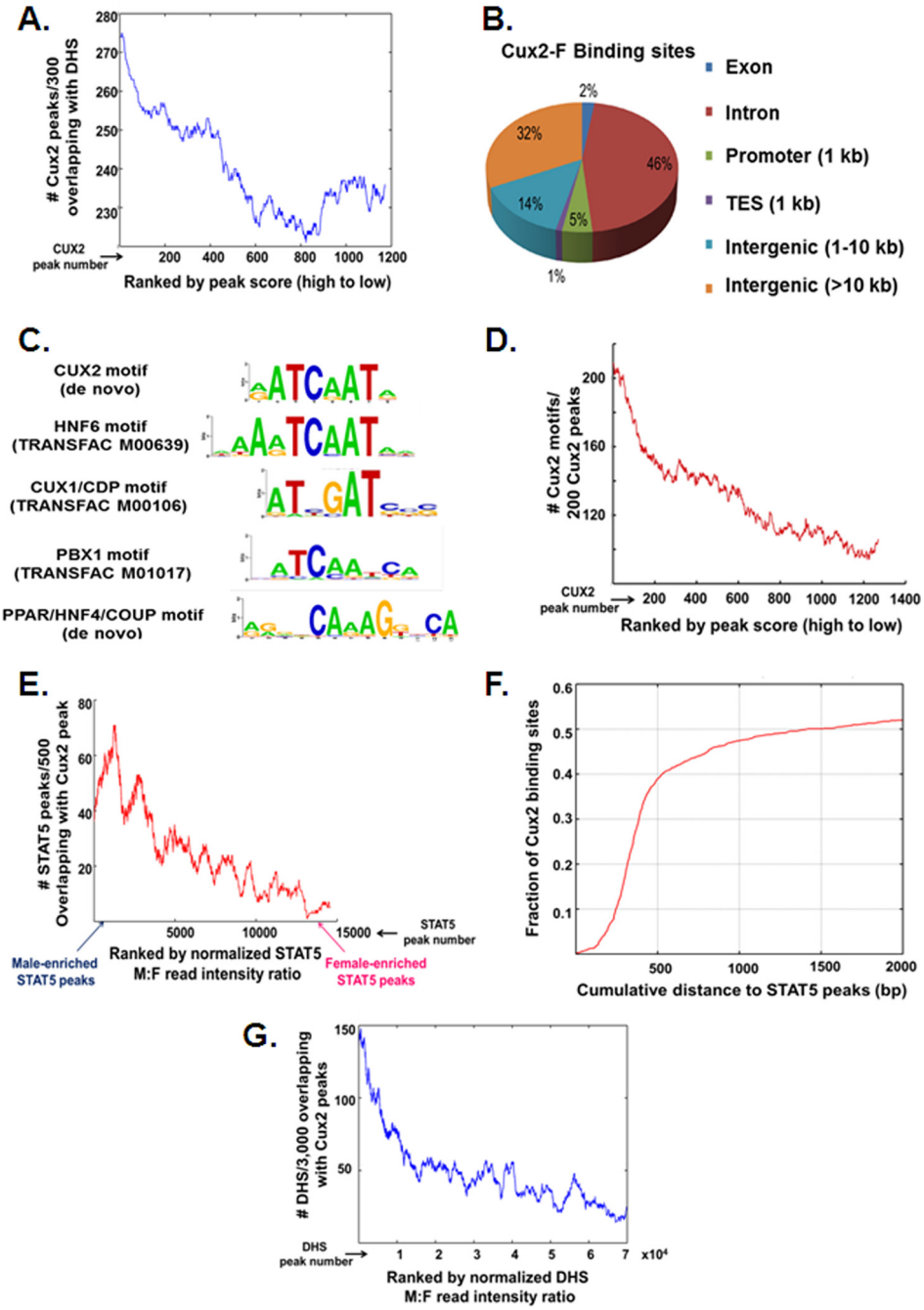

FIG 5 ChIP-Seq analysis of CUX2 binding sites in male and female mouse liver. (A) Number of CUX2 peaks, ranked by peak score, in each sequential set of 300 CUX2 peaks that overlap a DNase hypersensitivity site (DHS) (25), as a function of decreasing CUX2 peak MACS score. A total of 273 of the top 300 CUX2 peaks are at a DHS. (B) Distribution of CUX2 binding site locations (CUX2 peaks) relative to gene annotations. TES, transcript end site. (C) Shown are the primary *de novo*-discovered CUX2 motif, similar motifs in the Transfac database, and a secondary motif related to PPAR/HNF4/COUP. Also see Fig. S6 in the supplemental material. (D) Number of *de novo* CUX2 motifs in each sequential set of 200 CUX2 peaks, ranked by peak score, as a function of decreasing CUX2 peak MACS score. (E) Number of STAT5 ChIP-Seq peaks (54) that overlap a CUX2 peak in each sequential set of 500 STAT5 peaks, ranked as a function of the normalized STAT5 male/female read intensity ratio. (F) Proximity of CUX2 peaks to STAT5 ChIP-Seq peak using the merged set of 15,094 STAT5 peaks (54). (G) Number of DHSs in mouse liver (25) that overlap a CUX2 peak in each sequential set of 3,000 DHSs, ranked as a function of the normalized DHS male/female read intensity ratio.

Table S9B in the supplemental material). Thus, CUX2 binding is associated with CUX2-dependent gene repression but not with CUX2-dependent gene induction. Overall, 26% of CUX2 gene targets were altered in expression by adeno-CUX2 and/or CUX2 siRNA treatment (see Table S9B in the supplemental material), indicating that the CUX2 binding sites associated with these genes are functional with respect to regulation of gene expression. Although there was a significant depletion of CUX2 targets in genes induced by adeno-CUX2, a subset of female-biased CUX2 targets was associated with CUX2-dependent gene induction. Notable

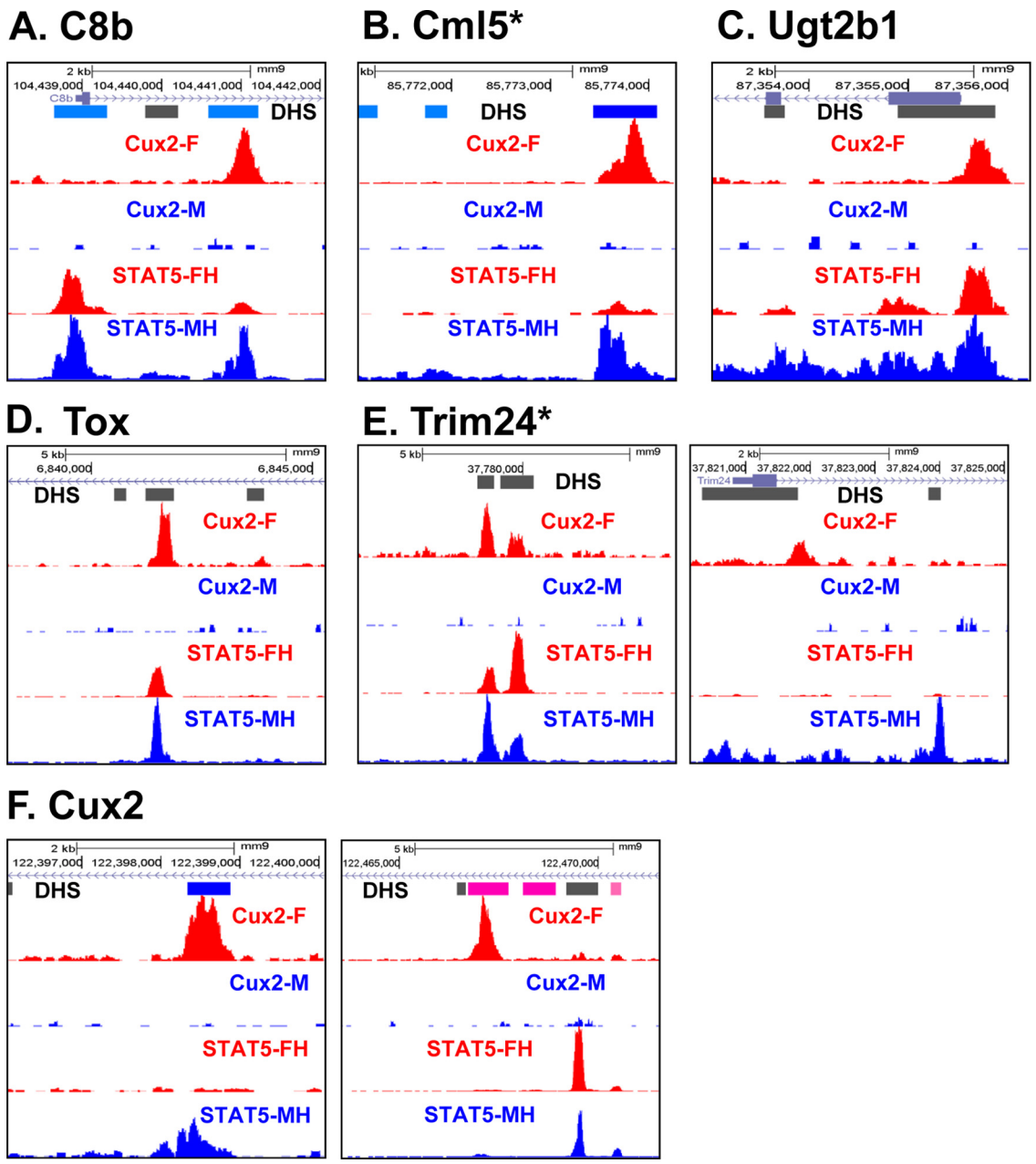

FIG 6 Sex-biased binding of CUX2 at sex-specific genes. Shown are UCSC Genome Browser screen shots of CUX2 and STAT5 binding within or near male-biased genes (*C8b*, *Cml5*, and *Ugt2b1*) (A to C) and female-biased genes (*Tox*, *Trim 24*, and *Cux2*) (D to F). High CUX2 binding is seen in female liver (CUX2-F) but not male liver (CUX2-M). Also shown are tracks of STAT5 binding in livers of male and female mice killed at a peak of STAT5 activity (STAT5-MH and STAT5-FH, respectively) (54), showing examples of CUX2 binding near STAT5 binding sites. Previously determined DNase I-hypersensitive sites are shown at the top as DHS; light blue bars represent male-specific DHSs, dark blue bars represent robust male-specific DHS binding sites, pink bars represent female-specific DHSs, and gray bars represent sex-independent DHSs. CUX2 peaks in female liver that overlap a male-biased STAT5 peak and a male-specific DHS genomic region were found near male-biased genes *C8b* and *Cml5* (A and B), whereas a CUX2 peak in *Ugt2b1* (C) overlapped peaks that displayed strong STAT5 binding in both male and female liver as well as a sex-independent DHS. CUX2 peaks near *Tox* (D) and *Trim24* (E) overlapped sex-independent DHSs and STAT5 peaks in both male and female liver. A peak in *Trim24* (right panel) was contained within a sex-independent DHS but did not overlap a STAT5 binding site. One of CUX2 peaks in the *Cux2* gene itself (F) overlapped a male-biased DHS that contains a male-biased STAT5 binding site, while another CUX2 peak coincided with a female-biased DHS. This second CUX2 peak did not overlap any STAT5 peaks, although a sex-independent STAT5 peak was located ~2.5 kb away. Asterisks indicate CUX2 peaks that are not within the gene; the CUX2 peak near *Cml5* is ~3 kb upstream, while the one near *Trim24* is ~42 kb upstream.

examples include six highly female-specific genes, all of which were induced by adeno-CUX2 in male liver and repressed by CUX2 siRNA in female liver (*A1bg*, *Cux2*, *Cyp2b9*, *Cyp3a44*, *Tox*, and *Trim24*) (see Table S9B in the supplemental material).

Transcriptional regulators altered by CUX2. We sought to identify transcription factors that might mediate the indirect (downstream) actions of CUX2. Thirty-four CUX2 target genes whose expression was altered by CUX2 overexpression or by

CUX2 knockdown were identified as transcriptional regulators by their Gene Ontology descriptors (see Table S10 in the supplemental material). One of these genes was *Cux2* itself, which is associated with 4 CUX2 binding sites. One of these sites is located in a region that is preferentially DNase hypersensitive and bound by STAT5 in male liver. The other three CUX2 binging sites overlap female-biased DNase-hypersensitive sites and are in the neighborhood of STAT5 binding sites occupied in either a female-biased or a sex-independent manner (Fig. 6F; see Table S9C in the supplemental material). Conceivably, *Cux2* expression may be repressed by STAT5 in male liver and subject to positive autoregulation in female liver. Other transcriptional regulator genes associated with multiple CUX2 binding sites include *Nfia* and *Onecut2* (4 binding sites each), *Pbx1* (3 sites), and *Bcl6* (2 sites). The last two encode transcription factors that are associated with GH regulation of liver sex differences (25, 33, 54). Fifty-three other transcriptional regulator genes that display sex-biased expression were identified as indirect targets of CUX2 (see Table S10 in the supplemental material). The overall set of 87 transcriptional regulators was enriched for homeobox proteins, zinc finger proteins, and factors related to muscle organ development (see Table S11 in the supplemental material). Seven of the sex-biased transcriptional regulators displayed the expected reciprocal responses to adeno-CUX2 and CUX2 siRNAs (see Table S10 in the supplemental material). Notably, 2 of the 7 genes, *Tox* and *Trim24*, show strong female-specific expression (23), are direct CUX2 targets, and were upregulated following overexpression of CUX2 in male liver and downregulated following CUX2 knockdown in female liver. For both genes, binding of CUX2 occurred at sex-independent DNase-hypersensitive sites (Fig. 6D and E). These findings indicate that CUX2 induces *Tox* and *Trim24* expression by a direct binding mechanism and suggest that one or both factors mediate the actions of CUX2 on its downstream targets.

CUX2 binding in postnatal versus young adult liver. CUX2 is expressed at similar levels in male and female mouse livers at 2 to 3 weeks of age, after which CUX2 levels decline ~20-fold in males but are increased ~2-fold in females (Fig. 4B), similar to the expression pattern in rat liver (23). These findings suggest that CUX2 contributes to the widespread changes in sex-biased gene expression that occur at puberty. Those changes primarily occur in male liver, where many male-biased genes are upregulated and female-biased genes are downregulated after 4 weeks of age (6). Given the transcriptional repressive activity of CUX2, we hypothesized that CUX2 binds to and represses a subset of male-biased genes in prepubertal male liver and that these genes are derepressed after 4 weeks of age, when CUX2 expression declines. Supporting this hypothesis, ChIP-qPCR analysis showed that CUX2 generally binds to its target genes at similar levels in livers of immature (2-week-old) male and female mice (Fig. 7A to F). Genes associated with few or no CUX2 ChIP-Seq reads (*Actb* and *Mdga2*) were used as negative controls (Fig. 7G and H). By 8 weeks of age, CUX2 binding was generally maintained or in some cases increased in female liver while decreasing to background levels in male liver, paralleling the downregulation of *Cux2* expression. These general patterns were seen at CUX2 binding sites associated with male-biased genes and also sex-independent genes (Fig. 7A and B versus C to F) and were independent of whether the binding site was located within a male-enriched or a sex-independent DNase-hypersensitive site (Fig. 7A to D versus E and F). The degree to which the levels of CUX2 binding changed between 2 weeks and 8 weeks varied from gene to gene, which could reflect developmental changes in chromatin structure and binding site accessibility.

Next, we examined whether genes altered by CUX2 overexpression are enriched for genes that show a developmental change in mouse liver between 3 and 8 weeks (6). Strikingly, 83% of the male-biased genes that were downregulated in adult male liver following adeno-CUX2 infection were upregulated in male liver from 3 to 8 weeks, consistent with CUX2 repressing these genes in prepubertal male liver (Fig. 8A). Unexpectedly, female-biased genes upregulated in female liver from 3 to 8 weeks also showed significant association with genes downregulated by CUX2 overexpression (Fig. 8B). This finding may reflect the ~20-fold overexpression of CUX2, which could lead to competition with transcriptional activators, such as HNF6, that does not normally occur in female liver. Stringent sex-independent genes induced by adeno-CUX2 were enriched in the sets of genes downregulated from 3 to 8 weeks, while stringent sex-independent genes repressed by adeno-CUX2 were enriched in the sets of genes upregulated from 3 to 8 weeks (Fig. 8C). No significant enrichment was found between genes altered by CUX2 siRNA and genes displaying a developmental change in expression from 3 to 8 weeks (data not shown), perhaps reflecting the incomplete knockdown of CUX2. Many genes showing developmental changes from 3 weeks to 8 weeks of age were unaffected by CUX2 overexpression (Fig. 8), indicating developmental regulation by mechanisms independent of CUX2.

DISCUSSION

Differences in pituitary GH secretion patterns between male (pulsatile secretion) and female (near-continuous secretion) mice and rats were discovered many years ago (16, 28) and play an essential role in the sex-specific expression of >1,000 genes in adult liver (49); however, the underlying molecular mechanisms of regulation by these divergent GH secretion patterns have only recently begun to be understood. GH-activated STAT5 preferentially binds nearby male-biased genes in male liver and nearby female-biased genes in female liver, enabling STAT5 to activate a substantial fraction of sex-biased genes in a sex-dependent manner (54). Moreover, a complex interplay between STAT5 and a STAT5-regulated transcriptional repressor, BCL6, contributes to the repression of female-biased genes in male liver (54). Presently, we show that a corresponding regulatory pathway is operative in female liver. This pathway involves CUX2, a GH-regulated, female liver-expressed homeobox protein with repressor activity that is not significantly expressed in male liver, where it is subject to negative regulation dependent on STAT5 and HNF4α (23). We identified genes that respond to overexpression of CUX2 in male liver, as well as genes whose expression is altered following CUX2 knockdown in female liver. In addition, CUX2 binding sites were identified using ChIP-Seq methodology and then mapped to putative CUX2 target genes. Together, our findings indicate that CUX2 regulates sex-biased genes in adult female liver by at least two major mechanisms: direct repression of a subset of male-biased genes and indirect activation of a subset of female-biased genes. In addition, we identified several notable examples of highly female-specific genes that are direct CUX2 targets subject to positive regulation by CUX2. The indirect effects of CUX2 are proposed to be mediated by one or more direct, female-specific CUX2 targets, two of which, the GH-regulated transcription fac-

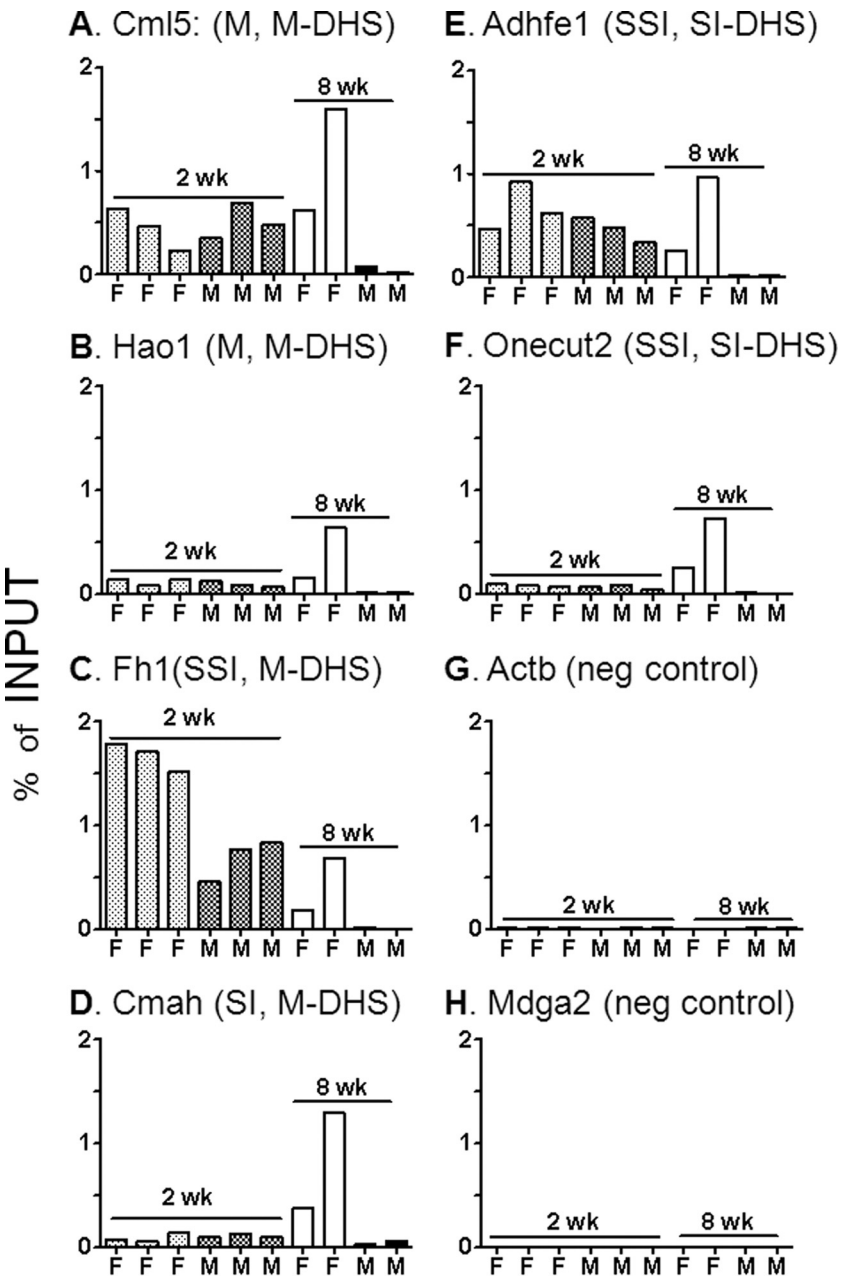

FIG 7 ChIP-qPCR analysis of CUX2 binding in 2-week and 8-week male and female mouse liver. Shown is CUX2 binding to sites identified by ChIP-Seq (see Table S9C in the supplemental material) near each of the indicated genes in individual 2-week-old and 8-week-old male and female mouse livers. Genes shown in panels A to F were all responsive to adeno-CUX2 and/or CUX2 siRNA (see Tables S2 and S3 in the supplemental material). M, male-biased gene; SI, sex-independent gene; SSI, stringent sex-independent gene; M-DHS, male-biased DNase-hypersensitive site; and SI-DHS, sex-independent DNase-hypersensitive site.

tors Tox and Trim24 (23), were identified as strong candidates (Fig. 9A). Finally, the present studies indicate a role for CUX2 in the postnatal regulation of many male-biased genes, which we propose are repressed by CUX2 in immature male and female liver and then selectively derepressed in male liver with the decline in CUX2 that begins after 2 to 3 weeks of age.

Liver responses to adeno-CUX2 and CUX2 siRNA. Adenovirus-mediated overexpression of CUX2 in adult male liver led to partial feminization of the liver transcriptome, with 35% of male-biased genes downregulated and 36% of female-biased genes upregulated. Much less frequently, we observed male-biased gene upregulation (2%) and female-biased gene downregulation (6%), highlighting the specificity of the above gene responses. Validating these results, we found that male-biased genes were preferentially upregulated and female-biased genes were preferentially downregulated in female liver following CUX2 knockdown using siRNA. Fewer genes responded to CUX2 knockdown than to CUX2 overexpression, which may reflect the incomplete knockdown of CUX2. The requirement for CUX2 overexpression to repress CUX2 gene targets in male liver may reflect competition

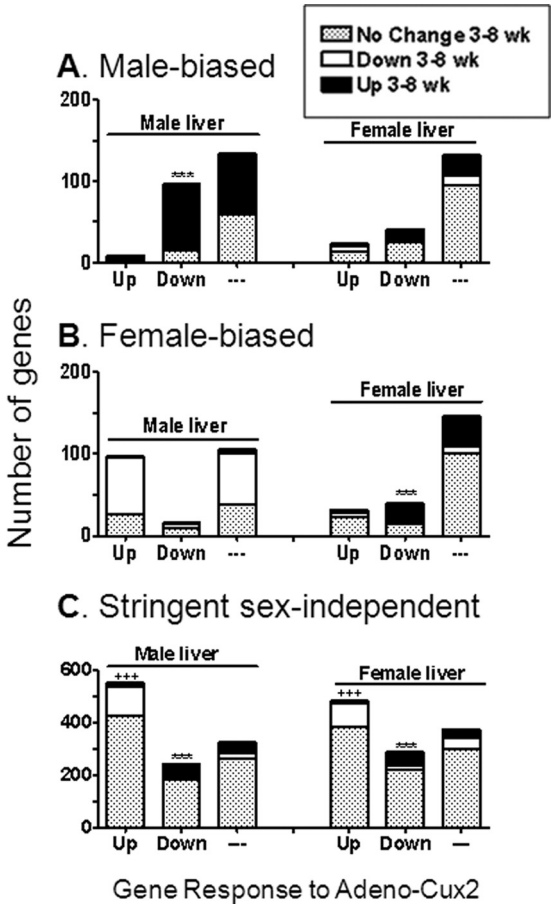

FIG 8 Genes responsive to CUX2 overexpression are enriched for genes showing developmental changes from 3 to 8 weeks. A comparison of male-biased (A), female-biased (B), and stringent sex-independent (C) genes altered by adeno-CUX2 treatment (5 days) to genes showing developmental changes between 3 weeks and 8 weeks in male (left) and female (right) mouse liver is shown. The developmental changes considered were upregulation, downregulation, and no change in expression from 3 weeks to 8 weeks at |fold change| > 1.5 and $P < 0.0001$, based on microarray studies reported elsewhere (6). Statistical analysis (two-tailed Fisher exact test): ***, ES $P < 10^{-5}$ for genes showing developmental upregulation from 3 to 8 weeks; +++, ES $P < 10^{-5}$ for genes showing development downregulation from 3 to 8 weeks.

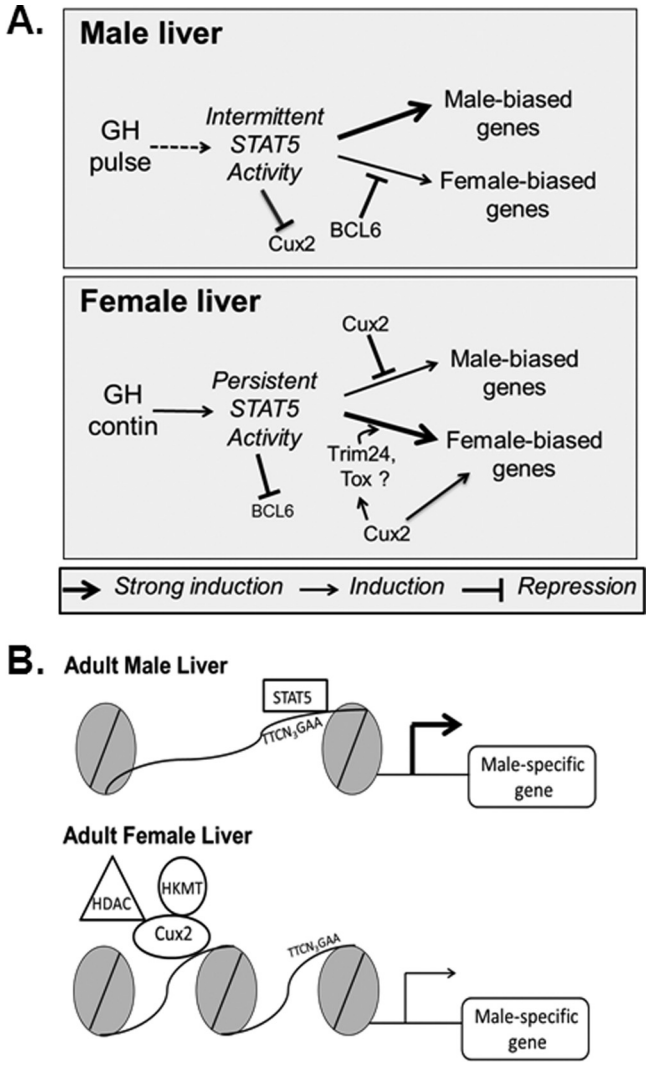

FIG 9 Model for regulation of sex-specific liver gene expression by CUX2. (A) Model for regulation of sex-biased genes in male and female liver. Differences in plasma GH secretion between males (pulsatile GH) and females (near-continuous GH) lead to sex-differential activation of STAT5 (pulsatile activation in male liver and persistent activation in female liver) and to male-biased expression of BCL6 and female-specific expression of CUX2 in mouse liver, as shown. BCL6 preferentially represses female-biased genes in male liver (54). In female liver, CUX2 represses 35% of male-biased genes, primarily through a direct binding mechanism. CUX2 also induces 36% of female-biased genes, acting through both direct and indirect mechanisms, with the direct CUX2 targets Tox and Trim24 potentially mediating these indirect effects. (B) Model for direct repression by CUX2 of male-biased genes in adult female liver. CUX2 binding sites in adult female liver are enriched at sites that are more open in male than in female liver (male-biased DNase hypersensitivity sites) that are also male-enriched STAT5 biding sites. CUX2 binding and recruitment of chromatin remodeling proteins, such as histone deacetylases (HDACs) and/or histone lysine methyltransferases (HKMTs), are proposed to alter chromatin accessibility and repress STAT5-dependent expression of male-biased target genes in female liver.

by positive-acting endogenous factors. One such factor is the transcriptional activator Onecut1/HNF6, whose motif is very similar to that of CUX2 and which likely competes with CUX2 for DNA binding. Other possibilities include the absence in male liver of a cofactor or a posttranslational modification required for efficient repression by CUX2 of its male-specific gene targets and the requirement of high levels of CUX2 to overcome the positive, stimulatory effects of male chromatin structure on male-specific gene expression.

Many fewer sex-specific genes responded to CUX2 overexpression in female liver than in male liver. This likely reflects the comparatively high endogenous female level of CUX2, which may be sufficient to maximally repress many male-biased genes, e.g., those whose basal expression is low. Indeed, genes repressed by adeno-CUX2 in both male and female liver tend to be more highly expressed in untreated female liver than genes repressed by adeno-CUX2 in male liver only (see Fig. S4 in the supplemental material).

While most genes responding to CUX2 overexpression in both male and female liver showed the same response in each sex, sex-dependent responses were seen in some cases. This may reflect a differential availability of transcriptional cofactors of CUX2, leading to the observed sex-differential regulation of these genes,

which are enriched in Gene Ontology terms such as cytochrome P450/monooxygenase activity, olfactory reception/G-coupled protein receptors, and muscle development/myofibril. Liver cytochromes P450 and other drug-metabolizing enzymes are well studied with respect to their impact on sex differences in pharmacology and toxicology (49).

CUX2 binding sites and target genes. ChIP-Seq was used to identify 1,471 CUX2 binding sites in female mouse liver and to map individual CUX2 binding sites to putative direct gene targets of CUX2 action. There was little or no significant specific CUX2 binding in male liver, consistent with CUX2 expression being highly female specific and validating the specificity of the CUX2 antibody. Greater than 80% of CUX2 binding sites coincided with open chromatin regions, which were identified by their hypersensitivity to DNase digestion. DNase hypersensitivity is a common characteristic of genomic regions associated with transcription factor binding and transcriptional regulation (25). Strikingly, the strong female-specific expression of CUX2 notwithstanding, CUX2 preferentially bound genomic regions that showed greater DNase hypersensitivity in male liver, rather than regions that showed greater hypersensitivity in female liver. Thus, CUX2 binds in female liver to chromatin regions that are significantly less open in female liver than in male liver (Fig. 9B). Moreover, CUX2 binding sites showed significant enrichment for genomic regions showing greater STAT5 binding in male liver, which are strongly associated with male-biased gene expression (54). In addition, a substantial fraction (40%) of CUX2 binding sites are located within 500 bp of a STAT5 peak summit, supporting the proposal that CUX2 action involves inhibition of STAT5-dependent male-biased gene expression (Fig. 9B). This mechanism is analogous to the repression of female-biased genes in male liver by the male-biased repressor BCL6 (33) (Fig. 9A) except that in the latter case BCL6 directly competes with STAT5 for DNA binding via their shared sequence motifs (54). Conceivably, CUX2 binding nearby STAT5 binding sites in association with chromatin-modifying enzymes may induce a change in chromatin structure that interferes with STAT5 binding and/or its ability to activate its male-biased gene targets (Fig. 9B). The related factor CUX1/CDP (48% amino acid sequence identity to CUX2) can bind nucleosomal DNA without disrupting the nucleosome core (21) and can repress gene expression by recruiting the histone deacetylase HDAC1 (24) and histone lysine methyltransferase G9a (36). Notably, 90% of the male-biased DNase-hypersensitive sites that overlap a CUX2 binding site are at least partially closed in response to continuous GH treatment (25), which represses many male-biased genes while inducing female-biased genes (12). Continuous GH treatment also induces CUX2 expression in male liver within 24 h (23), enabling CUX2 to bind to and repress these hypersensitive sites (putative enhancers) and thereby contribute to the observed feminization of the liver gene expression profile.

CUX2 binding sites were enriched near genes that are repressed by CUX2, implicating CUX2 in direct repression of these genes. In contrast, CUX2 binding sites were underrepresented in the set of genes induced by CUX2, indicating that CUX2 preferentially regulates members of the latter gene set in an indirect manner (Fig. 9A). However, only 26% of putative CUX2 target genes were responsive to adeno-CUX2 or CUX2 siRNA. This discrepancy may reflect the general difficulty in determining the true targets of bound transcription factors, some of which may act over long distances, as well as the possibility that some binding sites may be functionally irrelevant or redundant with other factors (29). A further factor may be the incomplete nature of some of our data sets (e.g., targets of CUX2 siRNA knockdown, as noted above). Moreover, the total number of CUX2 binding sites identified here is comparatively low: only 1,471 CUX2 sites, versus ≥5,000 to 10,000 genome-wide binding sites typically found for other liver transcription factors. This likely reflects the low titer of the available CUX2 antibody, which may yield chromatin complexes comprised of only the most populated CUX2 binding sites. Many CUX2 binding sites probably remain unidentified, and consequently, the preferential association between CUX2 binding and gene repression, but not gene activation, that we observed might not be fully representative of the actions of CUX2 genome-wide. Indeed, we found that CUX2 binds directly to several highly female-specific genes that are positively regulated by CUX2; these include *A1bg*, *Cyp2b9*, *Cyp3a44*, *Tox* and *Trim24*, and *Cux2* itself. Further studies will be required to ascertain the full extent to which CUX2 binding is associated with direct gene activation.

CUX2-regulated transcription factors. The transcription factors whose expression is CUX2 regulated include 11 homeobox and homeodomain-containing proteins (Cphx, CUX1, CUX2, Hmbox1, Onecut1/HNF6, Onecut2, PBX1, Prox1, Six1, Tgif2, and Zfhx4), which regulate development, differentiation, and other cellular processes (2, 45). Four of these factors (CUX1, Onecut1/HNF6, Onecut2, and Prox1) are involved in liver development (15, 18, 31), and binding sites for one of the factors (PBX1) are enriched at male-biased liver DNase-hypersensitive sites (25). PBX1 can serve as a cofactor of other homeodomain proteins (22, 38), while Tgif2 interacts with histone deacetylase I to repress gene expression (32). *Tgif2* was induced by overexpression of CUX2 and could play a role in CUX2 repression of male-biased genes by altering chromatin structure. Onecut1/HNF6 displays a binding site motif very similar to that of CUX2 (Fig. 5C), indicating that these two factors likely compete for binding to liver chromatin. Indeed, a large majority of the CUX2 binding sites identified here are also binding sites for HNF6 (unpublished experiments).

Two sex-specific transcriptional regulators identified as CUX2 targets, Tox and Trim24, showed reciprocal responses to CUX2 overexpression in male liver and CUX2 knockdown in female liver and may mediate the indirect stimulatory effects of CUX2 on female-biased genes (Fig. 9A). The female-specific expression of Tox and Trim24 requires GH and is dependent on two important global regulators of sex-specific liver gene expression, STAT5 and HNF4α (23). Tox is an HMG box protein that is expressed primarily in the thymus, liver, and brain (37). Trim24 can repress retinoic acid receptor transcriptional activity, and Trim24 deficiency in mice leads to increased retinoic acid signaling associated with development of hepatocellular carcinoma (11), which is more prevalent in male liver, where Trim24 is expressed at a low level compared to that in female liver (23). Accordingly, our finding that *Trim24* is positively regulated by CUX2 raises the possibility that CUX2 contributes to the Trim24-dependent protection from hepatocellular carcinoma. This contrasts with the liver cancer-stimulatory effects of the related factor CUX1, which lead to a more biologically aggressive phenotype in hepatocellular carcinoma (19).

Role of CUX2 in pubertal changes in sex-biased gene expression. Our findings suggest that CUX2 contributes to the large changes in expression of many sex-biased genes that occur in mouse liver at puberty (6). Genes showing male-biased expression

in adult liver are proposed to be repressed by CUX2 in immature liver, where CUX2 expression is high in both males and females; they are then selectively derepressed in male liver at puberty, when CUX2 expression is extinguished. Furthermore, since CUX2 can activate many adult female-biased genes, either directly or indirectly, CUX2 may support the expression of adult female-biased genes in immature male liver. Consistent with this proposal, CUX2 was bound to its target genes in both male and female liver at 2 weeks of age. Subsequently, CUX2 DNA binding was strongly repressed in male but not female liver at the time when many male-biased genes subject to negative regulation by CUX2 become activated. Substantial differences in the level of CUX2 binding in mouse liver chromatin at 2 weeks versus 8 weeks were apparent from one gene to the next (e.g., Fig. 7C versus D), which could be due to differences in chromatin structure or accessibility of these genes between immature and adult liver. The CUX2 direct target genes *Tox* and *Trim24* are upregulated in female liver and downregulated in male liver from 4 to 8 weeks and show female-biased expression at 4 weeks (6, 23), supporting the proposal that these factors mediate the indirect actions of CUX2 on female-biased gene expression during postnatal liver development. Finally, many adult male-biased genes that are upregulated from 3 to 8 weeks are apparently not regulated by CUX2, indicating that other factors and mechanisms regulate sex-biased genes during this developmental period. These factors likely include transcription factors and other signaling molecules that respond to the changes in pituitary GH secretion that occur around puberty and are essential for establishing adult patterns of sex-biased liver gene expression.

ACKNOWLEDGMENTS

This work was supported by National Institutes of Health grant DK33765 (to D.J.W.).

Microarray analysis was carried out at the Microarray and Bioinformatics Facility Core of the Environmental Health Sciences Center at Wayne State University, and high-throughput DNA sequence analysis was carried out at the BioMicro Center at MIT.

There are no competing interests to declare.

REFERENCES

1. **Akinc A, et al.** 2008. A combinatorial library of lipid-like materials for delivery of RNAi therapeutics. Nat. Biotechnol. **26**:561–569.
2. **Chariot A, Gielen J, Merville MP, Bours V.** 1999. The homeodomain-containing proteins: an update on their interacting partners. Biochem. Pharmacol. **58**:1851–1857.
3. **Chia DJ, Rotwein P.** 2010. Defining the epigenetic actions of growth hormone: acute chromatin changes accompany GH-activated gene transcription. Mol. Endocrinol. **24**:2038–2049.
4. **Choi HK, Waxman DJ.** 2000. Plasma growth hormone pulse activation of hepatic JAK-STAT5 signaling: developmental regulation and role in male-specific liver gene expression. Endocrinology **141**:3245–3255.
5. **Clodfelter KH, et al.** 2006. Sex-dependent liver gene expression is extensive and largely dependent upon signal transducer and activator of transcription 5b (STAT5b): STAT5b-dependent activation of male genes and repression of female genes revealed by microarray analysis. Mol. Endocrinol. **20**:1333–1351.
6. **Conforto TL, Waxman DJ.** 2012. Sex-specific mouse liver gene expression: genome-wide analysis of developmental changes from pre-pubertal period to young adulthood. Biol. Sex Differ. **3**:9.
7. **Cubelos B, et al.** 2010. Cux1 and Cux2 regulate dendritic branching, spine morphology, and synapses of the upper layer neurons of the cortex. Neuron **66**:523–535.
8. **Delesque-Touchard N, Park SH, Waxman DJ.** 2000. Synergistic action of hepatocyte nuclear factors 3 and 6 on CYP2C12 gene expression and suppression by growth hormone-activated STAT5b. Proposed model for female specific expression of CYP2C12 in adult rat liver. J. Biol. Chem. **275**:34173–34182.
9. **Eisen MB, Spellman PT, Brown PO, Botstein D.** 1998. Cluster analysis and display of genome-wide expression patterns. Proc. Natl. Acad. Sci. U. S. A. **95**:14863–14868.
10. **Gingras H, Cases O, Krasilnikova M, Berube G, Nepveu A.** 2005. Biochemical characterization of the mammalian Cux2 protein. Gene **344**: 273–285.
11. **Herquel B, et al.** 2011. Transcription cofactors TRIM24, TRIM28, and TRIM33 associate to form regulatory complexes that suppress murine hepatocellular carcinoma. Proc. Natl. Acad. Sci. U. S. A. **108**:8212–8217.
12. **Holloway MG, Laz EV, Waxman DJ.** 2006. Codependence of growth hormone-responsive, sexually dimorphic hepatic gene expression on signal transducer and activator of transcription 5b and hepatic nuclear factor 4alpha. Mol. Endocrinol. **20**:647–660.
13. **Huang DW, Sherman BT, Lempicki RA.** 2009. Bioinformatics enrichment tools: paths toward the comprehensive functional analysis of large gene lists. Nucleic Acids Res. **37**:1–13.
14. **Huang DW, Sherman BT, Lempicki RA.** 2009. Systematic and integrative analysis of large gene lists using DAVID bioinformatics resources. Nat. Protoc. **4**:44–57.
15. **Hulea L, Nepveu A.** 2012. CUX1 transcription factors: from biochemical activities and cell-based assays to mouse models and human diseases. Gene **497**:18–26.
16. **Jansson JO, Eden S, Isaksson O.** 1985. Sexual dimorphism in the control of growth hormone secretion. Endocrinol. Rev. **6**:128–150.
17. **Ji H, et al.** 2008. An integrated software system for analyzing ChIP-chip and ChIP-seq data. Nat. Biotechnol. **26**:1293–1300.
18. **Kamiya A, Kakinuma S, Onodera M, Miyajima A, Nakauchi H.** 2008. Prospero-related homeobox 1 and liver receptor homolog 1 coordinately regulate long-term proliferation of murine fetal hepatoblasts. Hepatology **48**:252–264.
19. **Kojima K, et al.** 2011. MicroRNA122 is a key regulator of alpha-fetoprotein expression and influences the aggressiveness of hepatocellular carcinoma. Nat. Commun. **2**:338.
20. **Lahuna O, et al.** 2000. Involvement of STAT5 (signal transducer and activator of transcription 5) and HNF-4 (hepatocyte nuclear factor 4) in the transcriptional control of the hnf6 gene by growth hormone. Mol. Endocrinol. **14**:285–294.
21. **Last TJ, van Wijnen AJ, de Ridder MC, Stein GS, Stein JL.** 1999. The homeodomain transcription factor CDP/cut interacts with the cell cycle regulatory element of histone H4 genes packaged into nucleosomes. Mol. Biol. Rep. **26**:185–194.
22. **Laurent A, Bihan R, Omilli F, Deschamps S, Pellerin I.** 2008. PBX proteins: much more than Hox cofactors. Int. J. Dev. Biol. **52**:9–20.
23. **Laz EV, Holloway MG, Chen CS, Waxman DJ.** 2007. Characterization of three growth hormone-responsive transcription factors preferentially expressed in adult female liver. Endocrinology **148**:3327–3337.
24. **Li S, et al.** 1999. Transcriptional repression of the cystic fibrosis transmembrane conductance regulator gene, mediated by CCAAT displacement protein/cut homolog, is associated with histone deacetylation. J. Biol. Chem. **274**:7803–7815.
25. **Ling G, Sugathan A, Mazor T, Fraenkel E, Waxman DJ.** 2010. Unbiased, genome-wide in vivo mapping of transcriptional regulatory elements reveals sex differences in chromatin structure associated with sex-specific liver gene expression. Mol. Cell. Biol. **30**:5531–5544.
26. **Love KT, et al.** 2010. Lipid-like materials for low-dose, in vivo gene silencing. Proc. Natl. Acad. Sci. U. S. A. **107**:1864–1869.
27. **Macisaac KD, et al.** 2006. A hypothesis-based approach for identifying the binding specificity of regulatory proteins from chromatin immunoprecipitation data. Bioinformatics **22**:423–429.
28. **MacLeod JN, Pampori NA, Shapiro BH.** 1991. Sex differences in the ultradian pattern of plasma growth hormone concentrations in mice. J. Endocrinol. **131**:395–399.
29. **MacQuarrie KL, Fong AP, Morse RH, Tapscott SJ.** 2011. Genome-wide transcription factor binding: beyond direct target regulation. Trends Genet. **27**:141–148.
30. **Mahony S, Benos PV.** 2007. STAMP: a web tool for exploring DNA-binding motif similarities. Nucleic Acids Res. **35**:W253–W258.
31. **Margagliotti S, et al.** 2007. The Onecut transcription factors HNF-6/OC-1 and OC-2 regulate early liver expansion by controlling hepatoblast migration. Dev. Biol. **311**:579–589.
32. **Melhuish TA, Gallo CM, Wotton D.** 2001. TGIF2 interacts with histone

deacetylase 1 and represses transcription. J. Biol. Chem. **276**:32109–32114.
33. **Meyer RD, Laz EV, Su T, Waxman DJ.** 2009. Male-specific hepatic Bcl6: growth hormone-induced block of transcription elongation in females and binding to target genes inversely coordinated with STAT5. Mol. Endocrinol. **23**:1914–1926.
34. **Michou AI, et al.** 1997. Adenovirus-mediated gene transfer: influence of transgene, mouse strain and type of immune response on persistence of transgene expression. Gene Ther. **4**:473–482.
35. **Mode A, Gustafsson JA.** 2006. Sex and the liver—a journey through five decades. Drug Metab. Rev. **38**:197–207.
36. **Nishio H, Walsh MJ.** 2004. CCAAT displacement protein/cut homolog recruits G9a histone lysine methyltransferase to repress transcription. Proc. Natl. Acad. Sci. U. S. A. **101**:11257–11262.
37. **O'Flaherty E, Kaye J.** 2003. TOX defines a conserved subfamily of HMG-box proteins. BMC Genomics **4**:13. doi:10.1186/1471-2164-4-13.
38. **Pineault N, Helgason CD, Lawrence HJ, Humphries RK.** 2002. Differential expression of Hox, Meis1, and Pbx1 genes in primitive cells throughout murine hematopoietic ontogeny. Exp. Hematol. **30**:49–57.
39. **Rajagopalan D.** 2003. A comparison of statistical methods for analysis of high density oligonucleotide array data. Bioinformatics **19**:1469–1476.
40. **Saldanha AJ.** 2004. Java Treeview–extensible visualization of microarray data. Bioinformatics **20**:3246–3248.
41. **Severgnini M, et al.** 2012. A rapid two-step method for isolation of functional primary mouse hepatocytes: cell characterization and asialoglycoprotein receptor based assay development. Cytotechnology **64**:187–195.
42. **Soutschek J, et al.** 2004. Therapeutic silencing of an endogenous gene by systemic administration of modified siRNAs. Nature **432**:173–178.
43. **Tannenbaum GS, Choi HK, Gurd W, Waxman DJ.** 2001. Temporal relationship between the sexually dimorphic spontaneous GH secretory profiles and hepatic STAT5 activity. Endocrinology **142**:4599–4606.
44. **Veldhuis JD.** 1998. Neuroendocrine control of pulsatile growth hormone release in the human: relationship with gender. Growth Horm. IGF Res. **8**(Suppl. B):49–59.
45. **Vershon AK.** 1996. Protein interactions of homeodomain proteins. Curr. Opin. Biotechnol. **7**:392–396.
46. **Walker SR, Nelson EA, Frank DA.** 2007. STAT5 represses BCL6 expression by binding to a regulatory region frequently mutated in lymphomas. Oncogene **26**:224–233.
47. **Wauthier V, Sugathan A, Meyer RD, Dombkowski AA, Waxman DJ.** 2010. Intrinsic sex differences in the early growth hormone responsiveness of sex-specific genes in mouse liver. Mol. Endocrinol. **24**:667–678.
48. **Wauthier V, Waxman DJ.** 2008. Sex-specific early growth hormone response genes in rat liver. Mol. Endocrinol. **22**:1962–1974.
49. **Waxman DJ, Holloway MG.** 2009. Sex differences in the expression of hepatic drug metabolizing enzymes. Mol. Pharmacol. **76**:215–228.
50. **Waxman DJ, Ram PA, Park SH, Choi HK.** 1995. Intermittent plasma growth hormone triggers tyrosine phosphorylation and nuclear translocation of a liver-expressed, Stat 5-related DNA binding protein. Proposed role as an intracellular regulator of male-specific liver gene transcription. J. Biol. Chem. **270**:13262–13270.
51. **Weng L, et al.** 2006. Rosetta error model for gene expression analysis. Bioinformatics **22**:1111–1121.
52. **Wiwi CA, Waxman DJ.** 2004. Role of hepatocyte nuclear factors in growth hormone-regulated, sexually dimorphic expression of liver cytochromes P450. Growth Factors **22**:79–88.
53. **Xu J, et al.** 2011. Exploring endocrine GH pattern in mice using rank plot analysis and random blood samples. J. Endocrinol. **208**:119–129.
54. **Zhang Y, Laz EV, Waxman DJ.** 2012. Dynamic, sex-differential STAT5 and BCL6 binding to sex-biased, growth hormone-regulated genes in adult mouse liver. Mol. Cell. Biol. **32**:880–896.
55. **Zhang Y, et al.** 2008. Model-based analysis of ChIP-Seq (MACS). Genome Biol. **9**:R137. doi:10.1186/gb-2008-9-9-r137.